KAGRA observation run: performance of the Type A suspensions

L. Trozzo on behalf of VIS team

ICRR Institute for Cosmic Ray Research University of Tokyo

東京大学 THE UNIVERSITY OF TOKYO

OUTLINE

- Introduction
- Seismic noise
- Type A
- TypeA: sensor noise characterisation
- Sensor Correction (SC): noise budget
- Type GAS filters: EY case
- KAGRA low frequency sensitivity
    - Type A mechanical noise
    - Type A performance
- Conclusions

Introduction to KAGRA

KAGRA is the first kilometric gravitational-wave (GW) detector to be **underground** and **cryogenic.** It is an ITF Michelson interferometer with 3 Km Fairy-Perot arm cavities aiming to detect GW starting from 10 Hz.

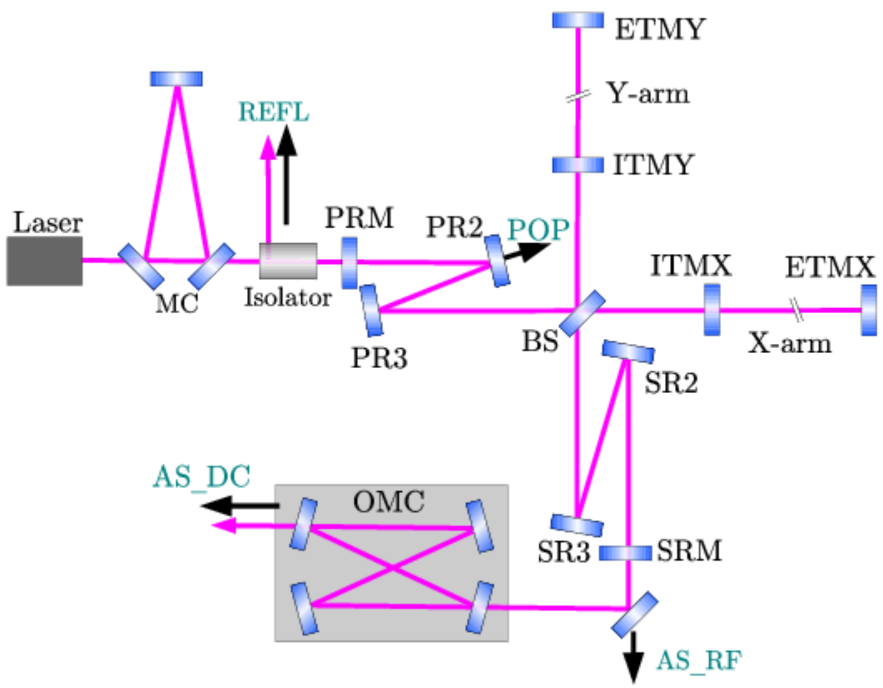

Target sensitivity of KAGRA

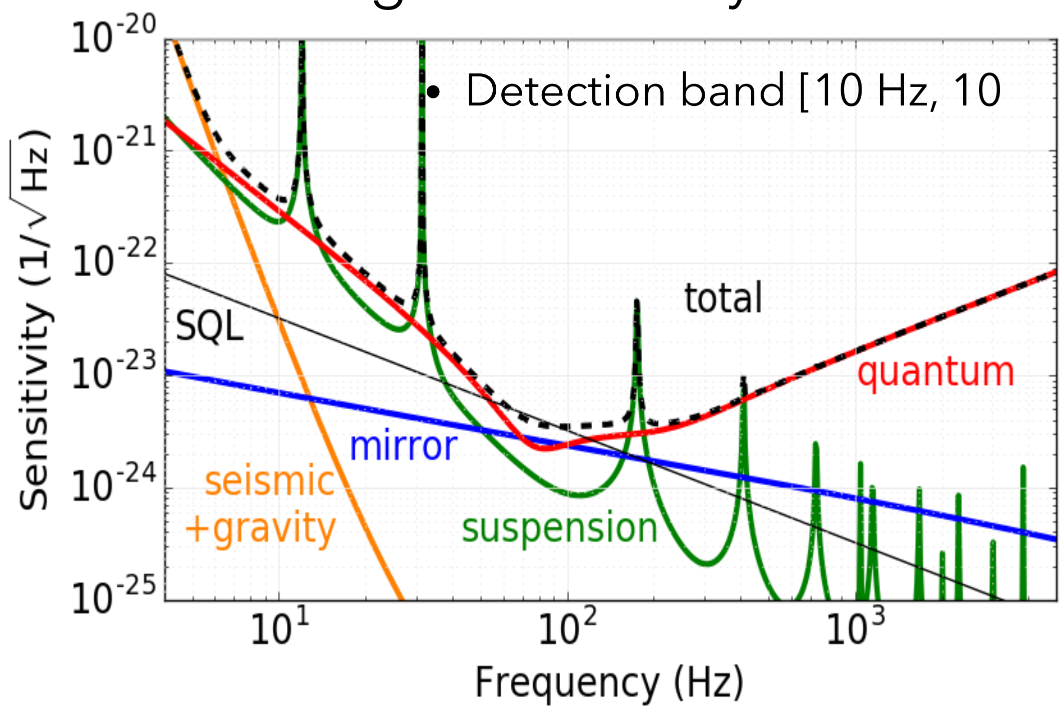

Limitations: Seismic Noise, Shot Noise, Thermal Noise.

Underground

Reduce Seismic Noise

Cryogenic

Reduce Thermal Noise

KAGRA first observation run (as PRFPMI interferometer) started last February 24 and ended up on April 21

Experience with underground operation is particularly interesting as next generation GW detector are planned to be underground.

The performance of the type A suspensions and their impact on the sensitivity curve when different microseismic conditions occur, during the KAGRA observation run will be analysed.

Seismic noise

KAGRA has been designed to be sensitive to GW starting from 10 Hz.

❋ Seismic noise: is the dominant noise at low frequencies (below 10 Hz):

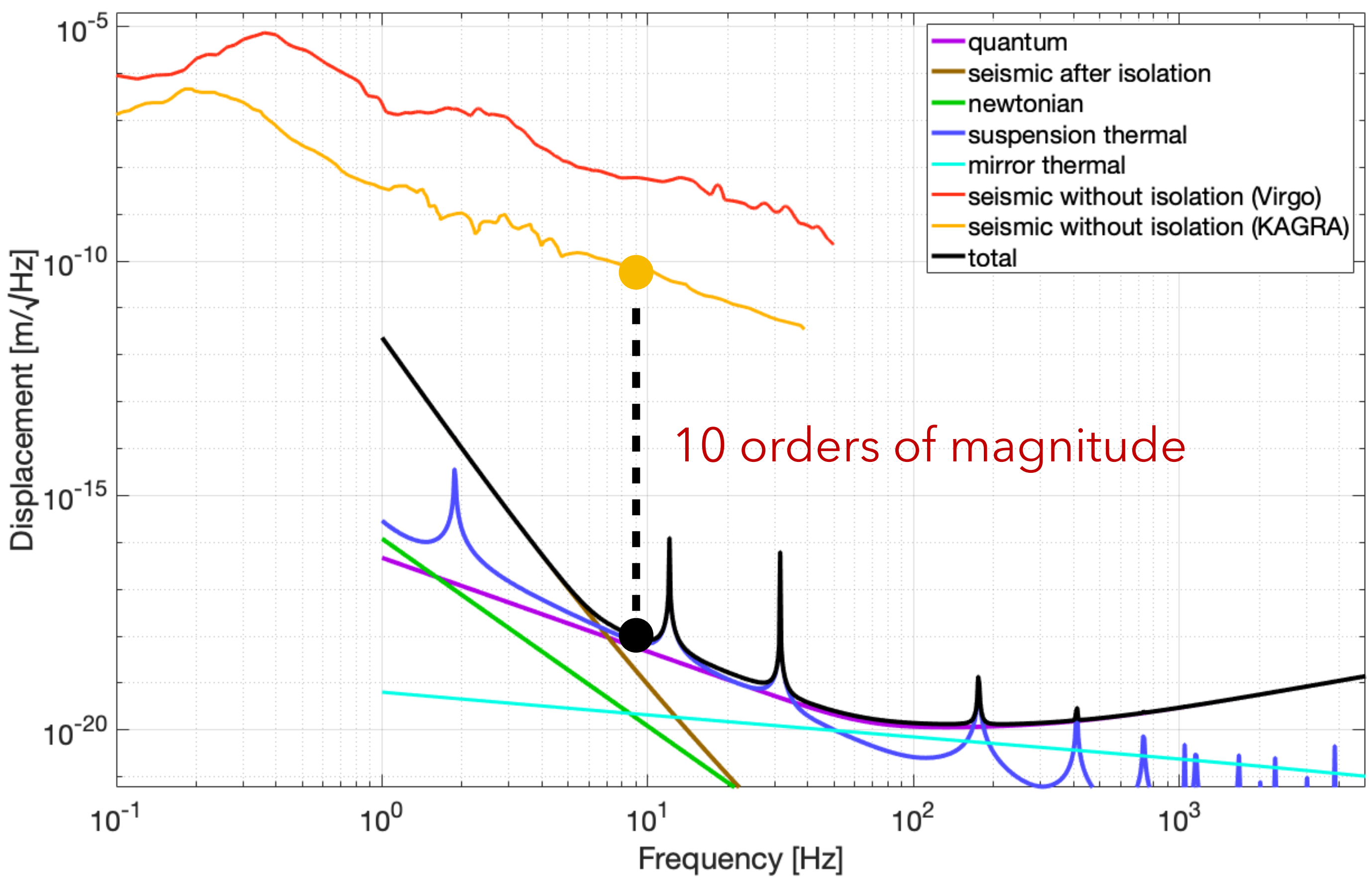

❋ In detection band > 10 Hz the seismic noise reaches the values

On surface

$$\frac{10^{-9}m}{\sqrt{Hz}}$$

Underground

$$\frac{10^{-11}m}{\sqrt{Hz}}$$

To detect the small distance variation due to GW

$$\frac{10^{-18}m}{\sqrt{Hz}}$$

A seismic isolation with a high attenuation capability ~ 10 orders of magnitude is required!

- **Free-falling TM (Test Mass)**
- **Isolation from Seismic Noise**

→ **Type A suspensions**

Type A suspensions

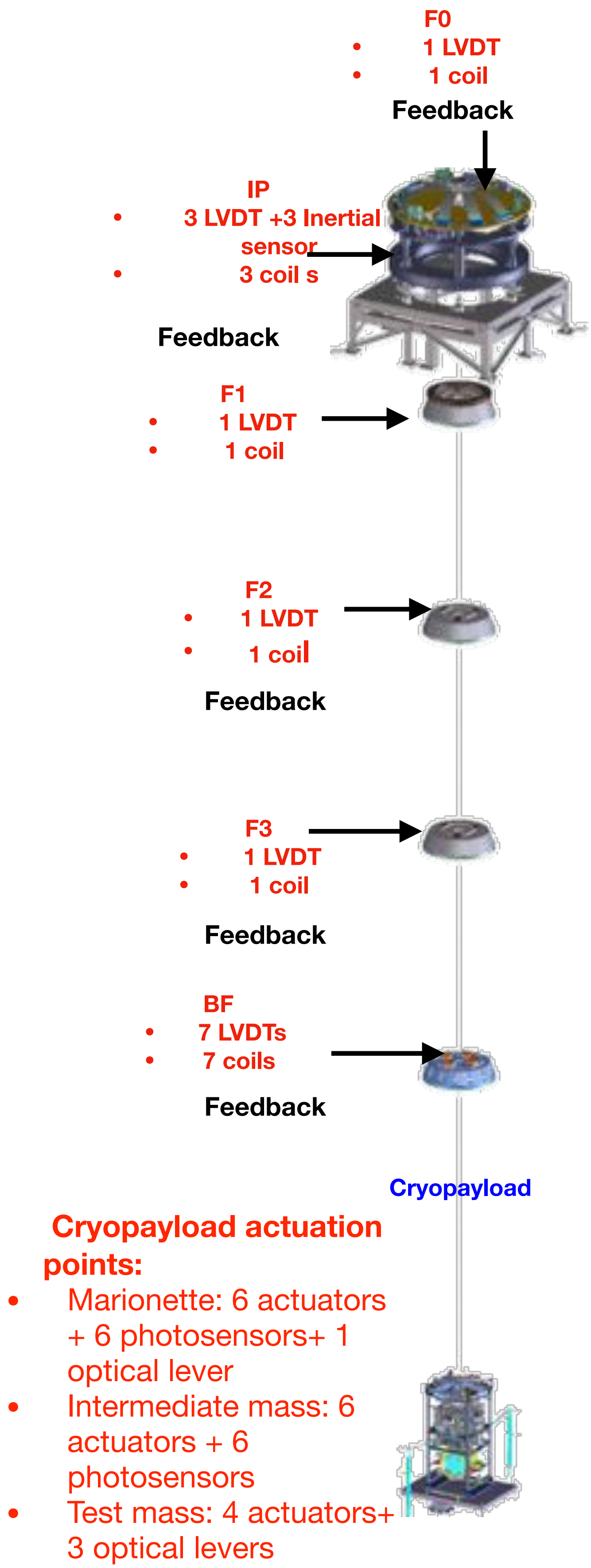

Type A are a nine-stage pendulum with the height of 13.5 m, whose top-stage loaded on a short inverted pendulum

The **Inverted Pendulum (IP)** and the **first vertical stage (F0)** fixed at its top are often considered as a pre-isolators, but their main role is that of letting actuated DC and damping control

The **suspension chain** consists of cascaded geometric anti-spring filters that show low frequency mechanical resonances.

The bottom four stages including the sapphire mirror are called **cryogenic payload** and cooled down to about 20 K in order to reduce the thermal noises.

The normal modes of the pendulum mechanical structure (tower part) are confined in low frequency region (below 2 Hz)

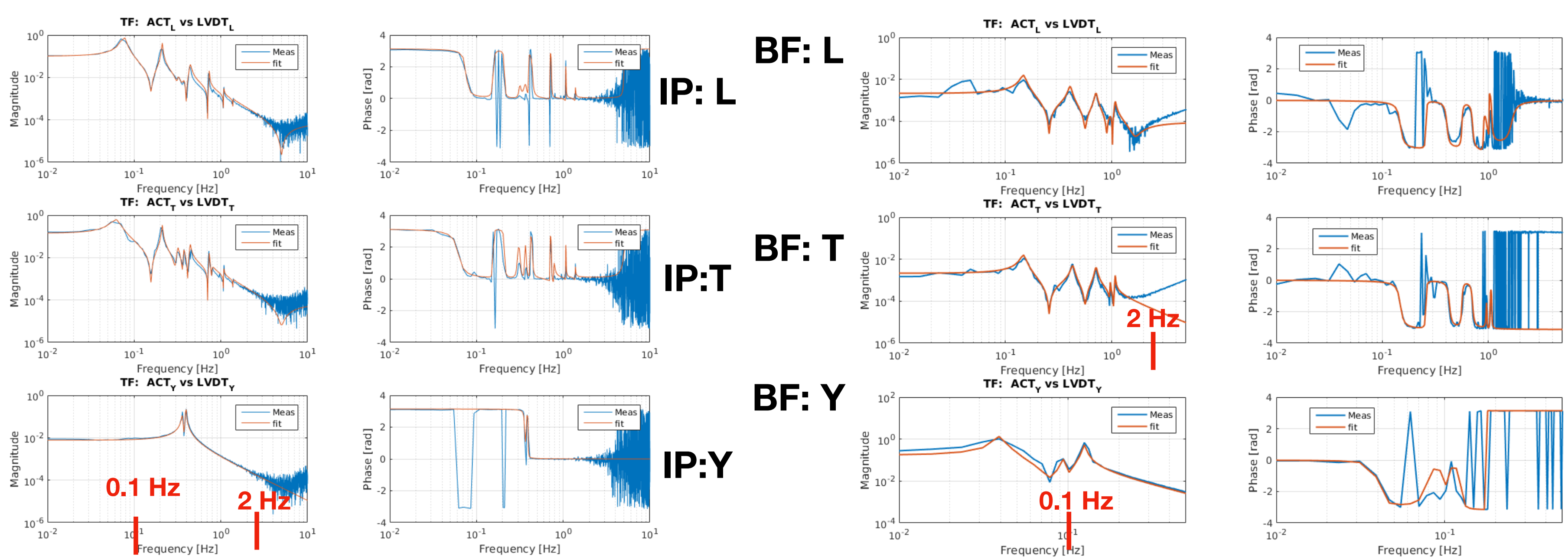

Type A: sensor noise characterisation (I)

Sensors spectrum signal (LVDT, accelerometer, geophone) versus intrinsic noise (model)

LVDT: noise budget

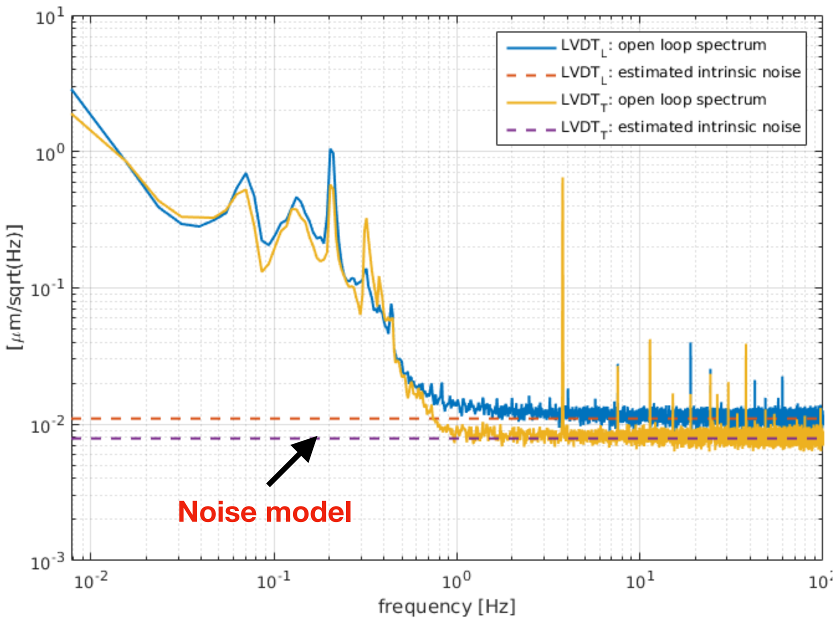

Accelerometer: noise budget

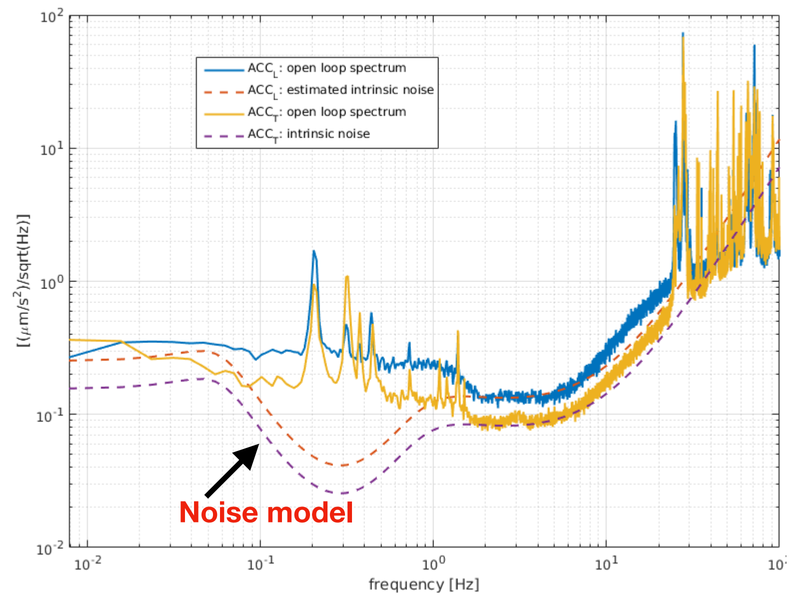

Geophone: noise budget

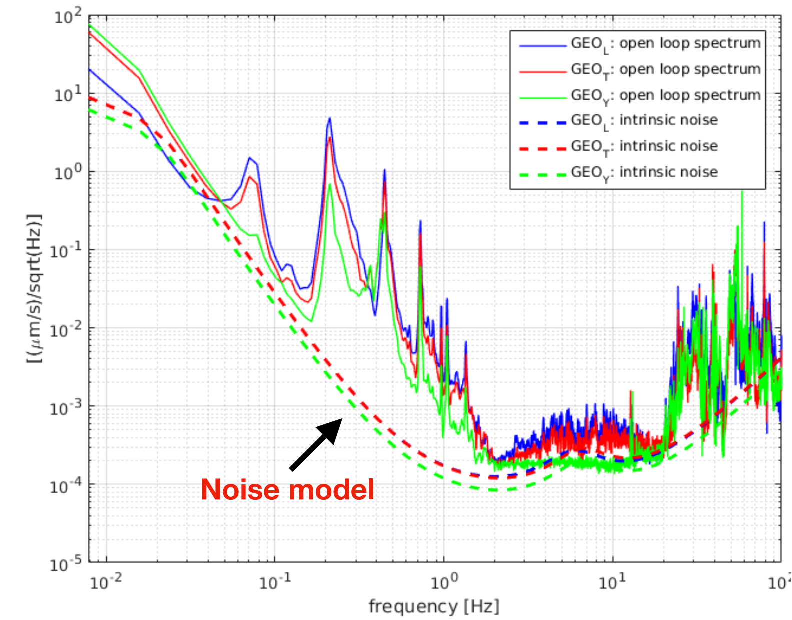

L,T,Y base

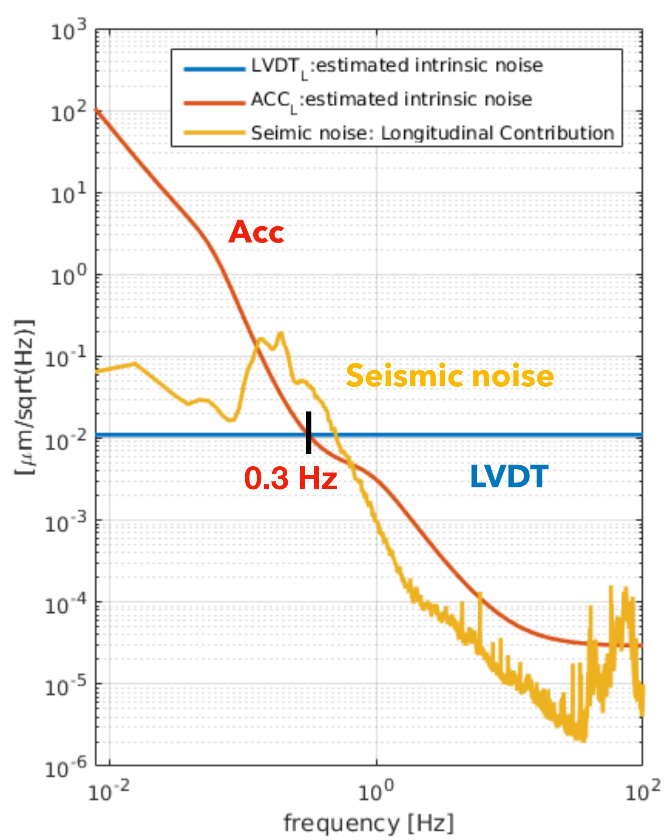

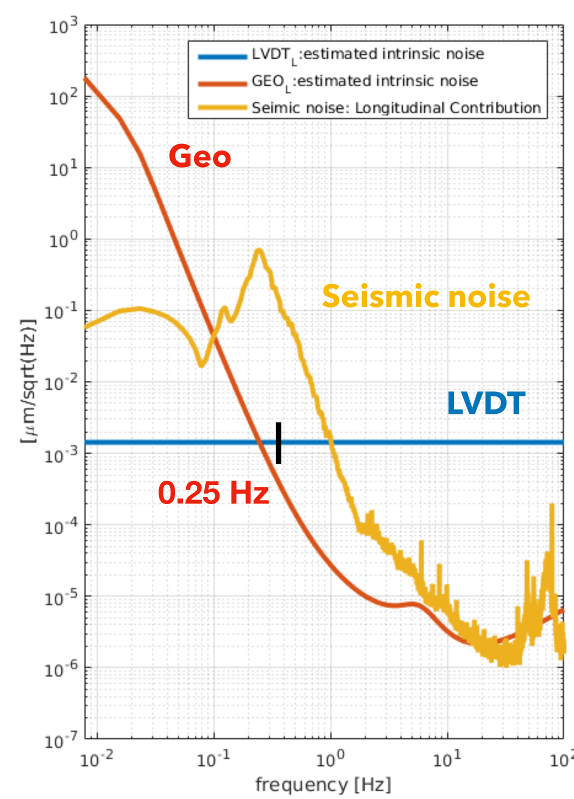

In the range [0.1,0. 5] Hz,] microseismic noise is dominant

Below 0.3 mHz, the accelerometer noise is dominant

Below 0.250 mHz, the geophone noise is dominant

To suppress the re-injection of microseismic noise

- **Blending technique**
- **Sensor Correction**

Type A: sensor noise characterisation (II)

- **Blending technique**

To take the better part of both signals, the blended virtual sensor, is attained through neutral pre-filtering:

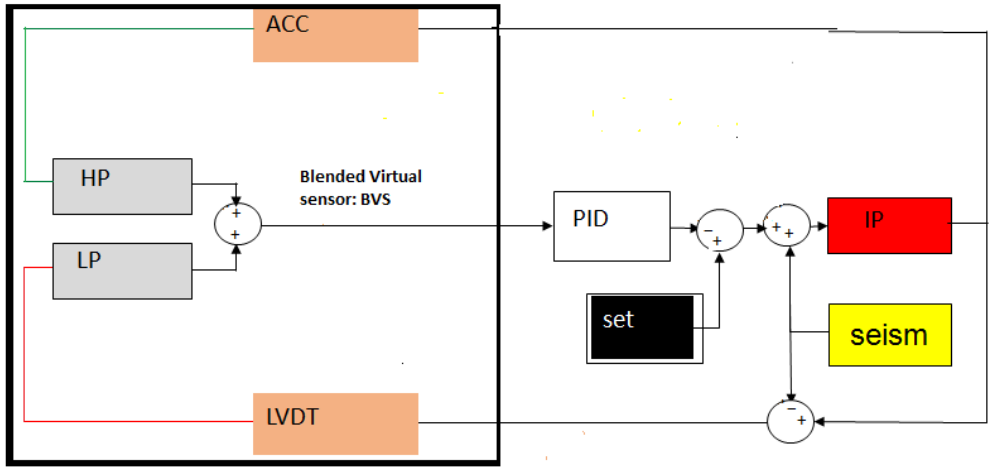

ACC or GEO
High Pass filter (HP)

LVDT
Low Pass filter (LP)

HP+LP=1

$$S(\omega) = LP(\omega) \cdot S_{LVDT}(\omega) - \omega^2 \cdot HP(\omega) \cdot S_{acc}(\omega)$$

- **Sensor correction**

The virtual sensor is attained through the subtraction of the seismic noise (measured by seismometer) and the LVDT signal

$$S(\omega) = S_{LVDT}(\omega) - HP_{SC}(\omega) \cdot S_{seim}(\omega)$$

Typical shape TF from ground to LVDT

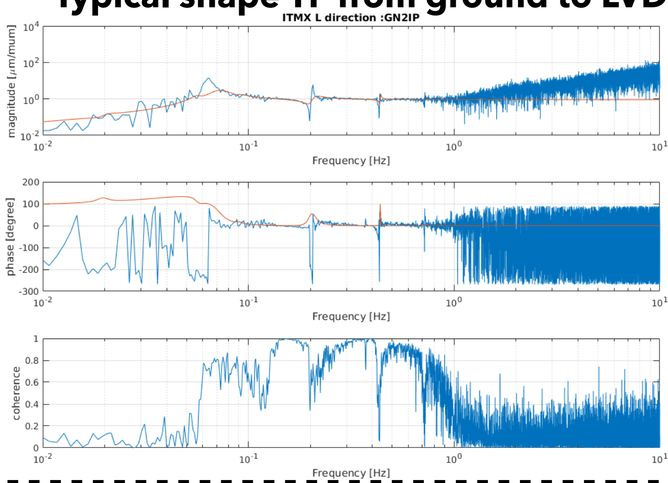

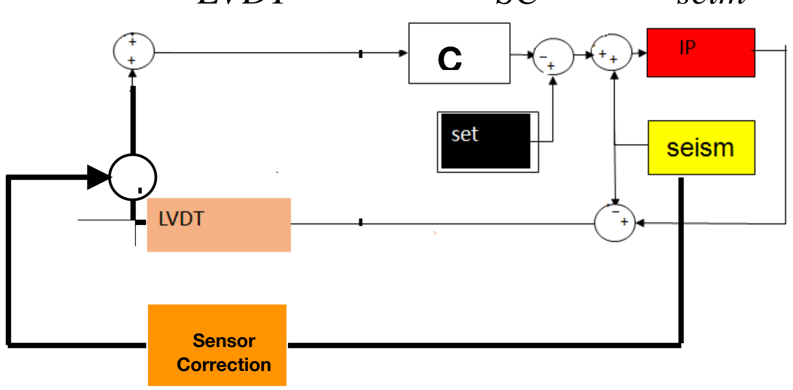

Typical shape HP filter

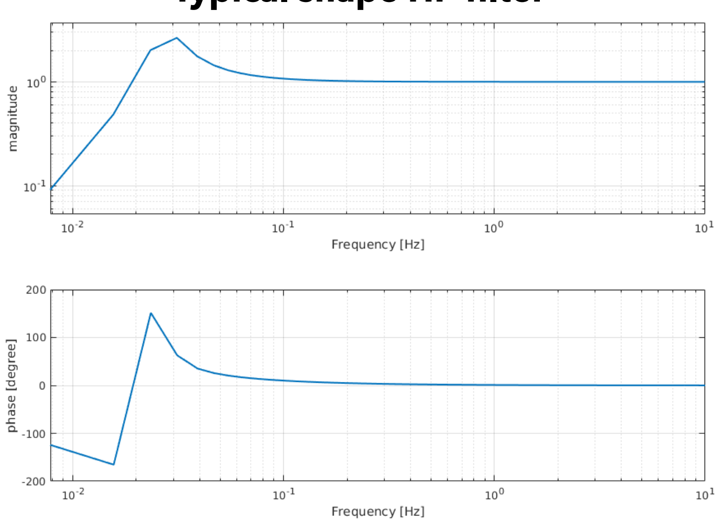

Type A: sensor noise characterisation (III)

$$S(\omega) = LP(\omega) \cdot S_{LVDT}(\omega) - \omega^2 \cdot HP(\omega) \cdot S_{acc}(\omega)$$

- **Blending technique**

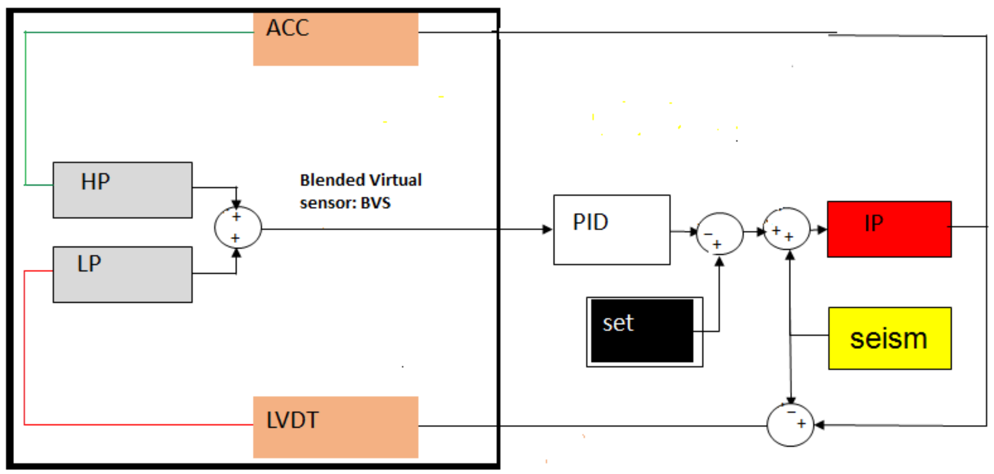

In this configuration three sources of noise can be identified:

- **LVDT noise (l)**
- **Seismic noise (S)**
- **Inertial sensor noise (g)**

- **Sensor Correction technique**

$$S(\omega) = S_{LVDT}(\omega) - HP_{SC}(\omega) \cdot S_{seim}(\omega)$$

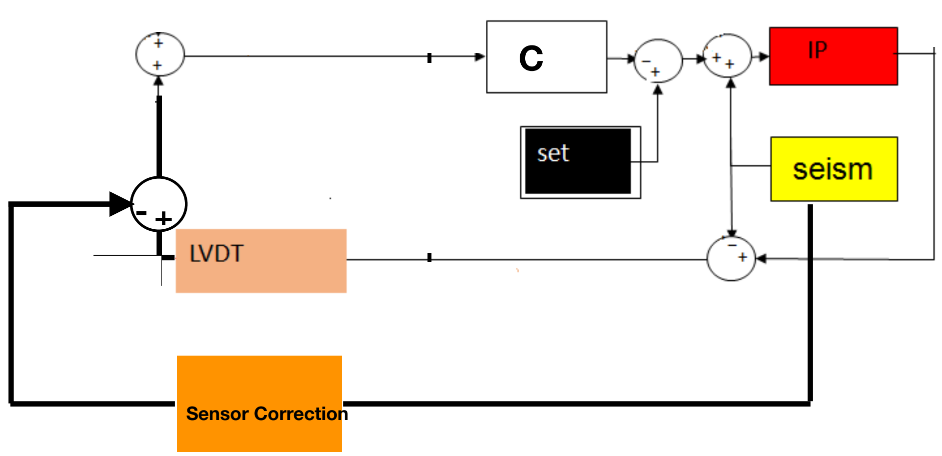

In this configuration three sources of noise can be identified:

- **LVDT noise (l)**
- **Seismic noise (S)**
- **Seismometer noise(g)**

Type A: sensor noise characterisation (IV)

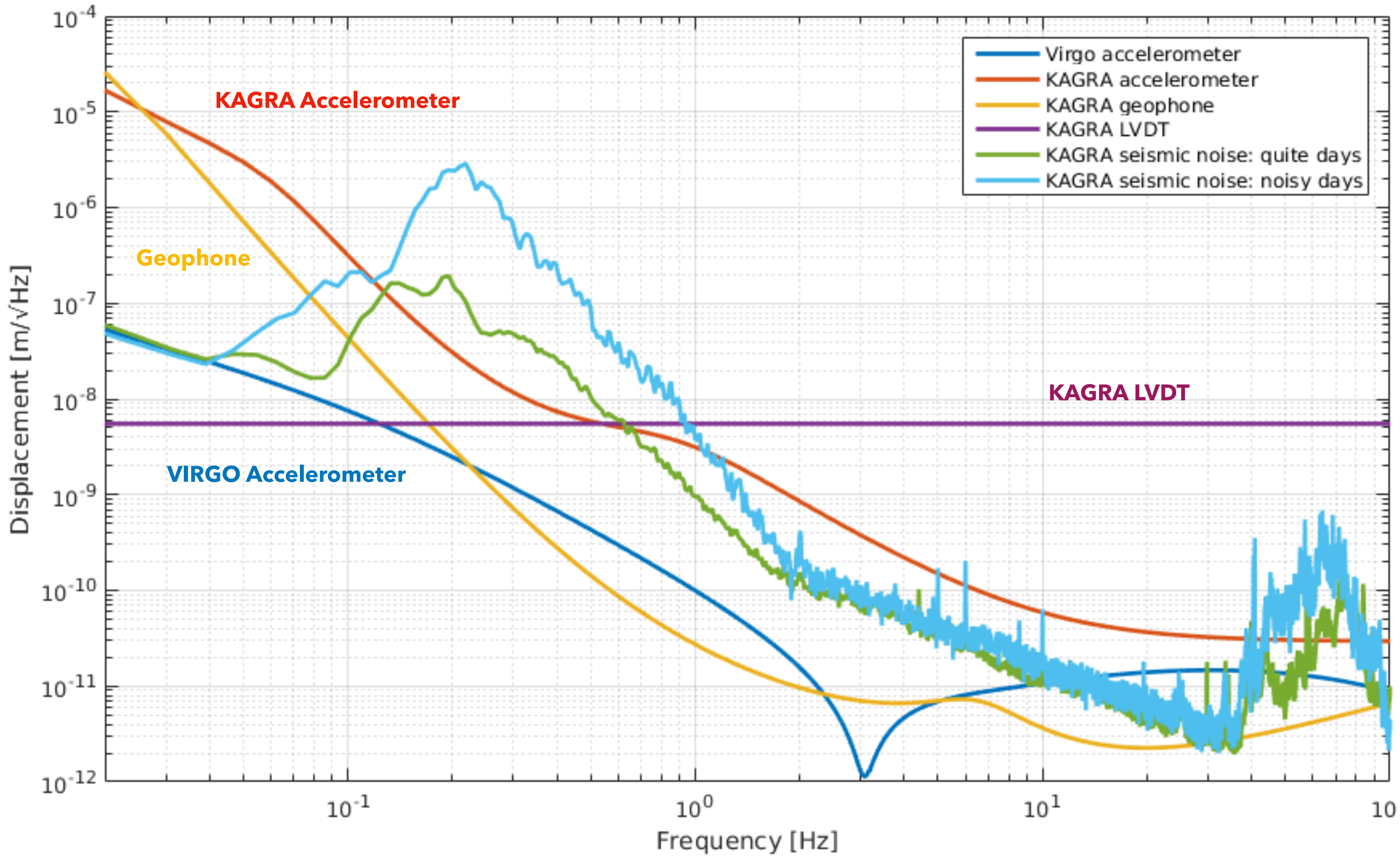

<u>At 0.150 Hz the Kagra Inertial sensors are to noisy compared with Virgo one</u>

<u>1) the geophone shows high DC noise and strange phase response below 0.1 Hz (</u> http://klog.icrr.u-tokyo.ac.jp/osl/?r=10334 ***)***

<u>2) KAGRA accelerometer shows high DC noise. Despite this it was stable with blending @ 90 mHz (</u>http://klog.icrr.u-tokyo.ac.jp/osl/?r=7395***)***

<u>The noise of the inertial sensor is re-injected via loop causing the grow in up of the peak @ 0.148 Hz: this means that the loop is exciting the test mass at that frequency and is hard to lock the ITF.</u>

<u>It is hard to blend below 0.09 Hz</u>

Type A: sensor noise characterisation (V)

$$S(\omega) = LP(\omega) \cdot S_{LVDT}(\omega) - \omega^2 \cdot HP(\omega) \cdot S_{acc}(\omega)$$

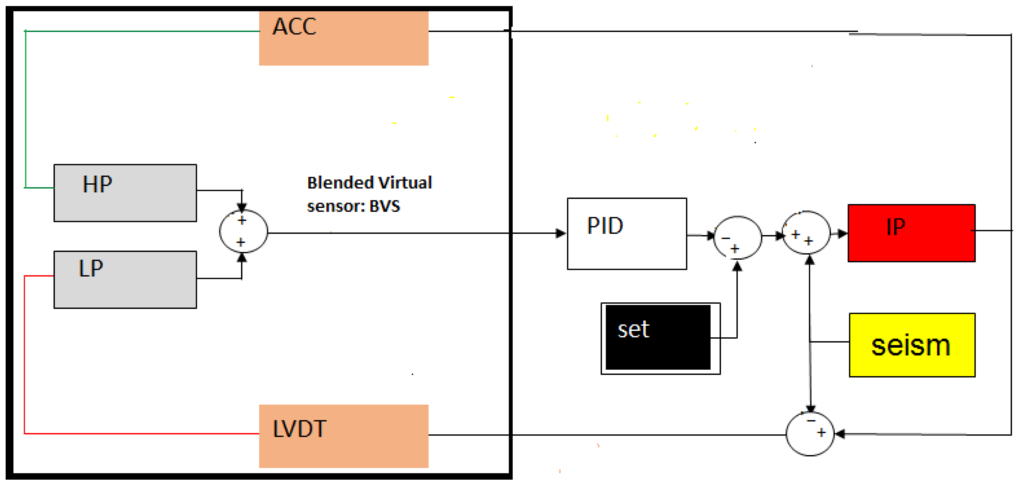

- **Blending technique: sum of the noise**

Let's assume that these noise are uncorrelated:

$$S_{noise} = \sqrt{(LP \cdot l)^2 + (HP \cdot g)^2 + (LP \cdot S)^2}$$

***All units are displacement**

$$S(\omega) = S_{LVDT}(\omega) - HP_{SC}(\omega) \cdot S_{seim}(\omega)$$

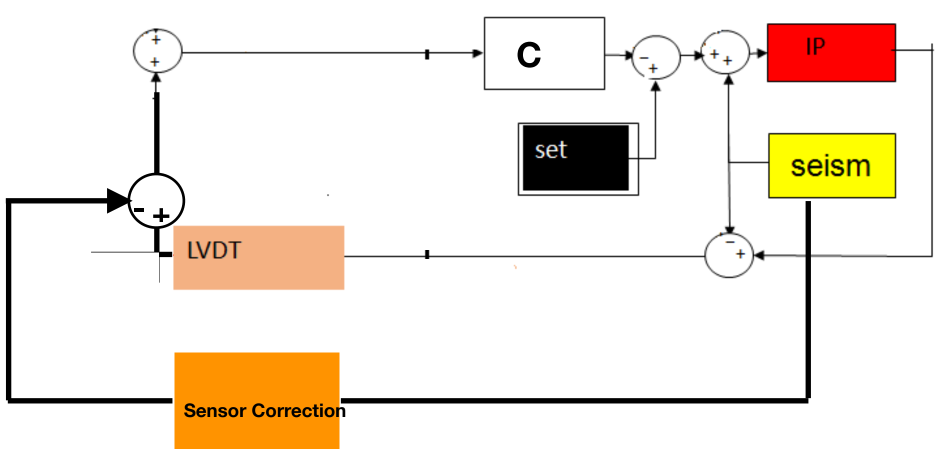

- **Sensor Correction: sum of the noise**

Let's assume that these noise are:

- *uncorrelated*
- *g<<S*

$$S_{noise} = \sqrt{l^2 + ((1 - HP) \cdot S)^2}$$

Type A: sensor noise characterisation (VI)

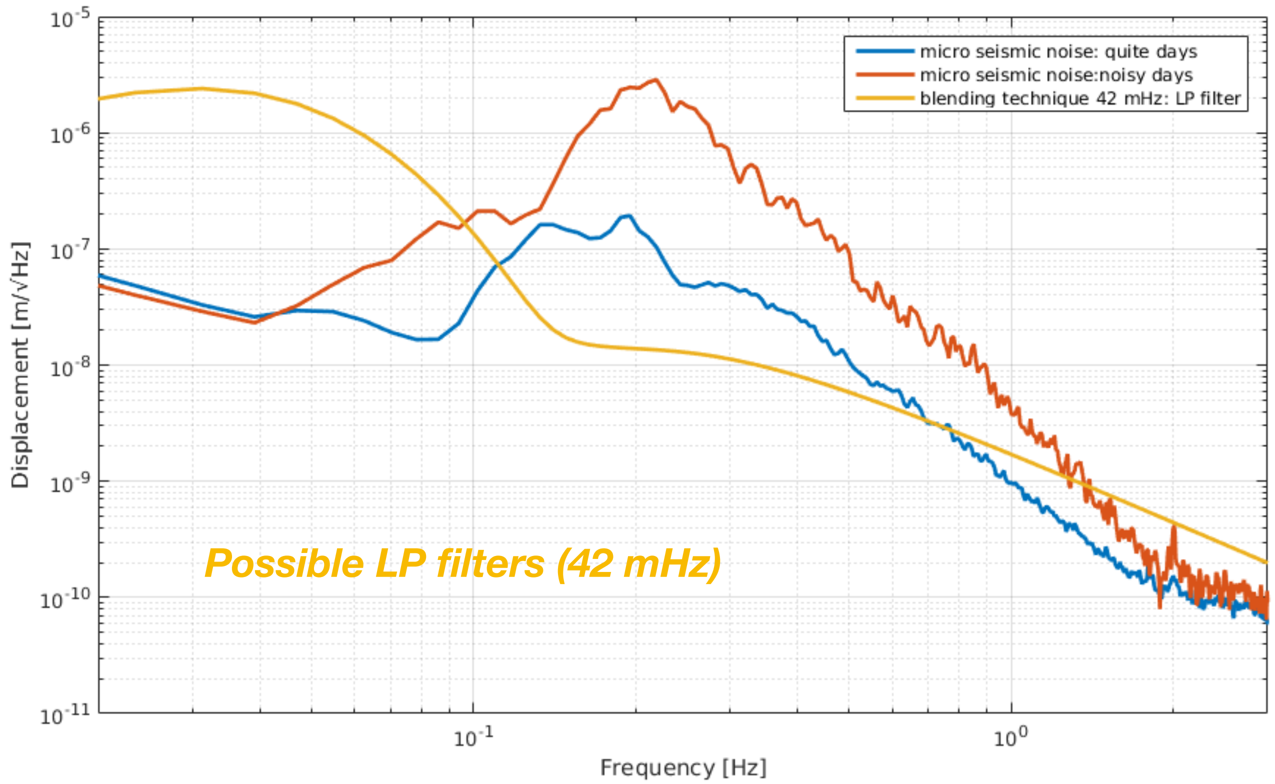

- *LP filter has been shaped taking into account the background disturbance (seismic noise)*
- *For LP filter tipical cutoff is below 100 mHz, to reduce the seismic contribution.*
- *For HP filter should be careful design so not to reintroduce accelerometer noise.*

Evaluation of the microseismic noise re-injection via blending technique and sensor correction

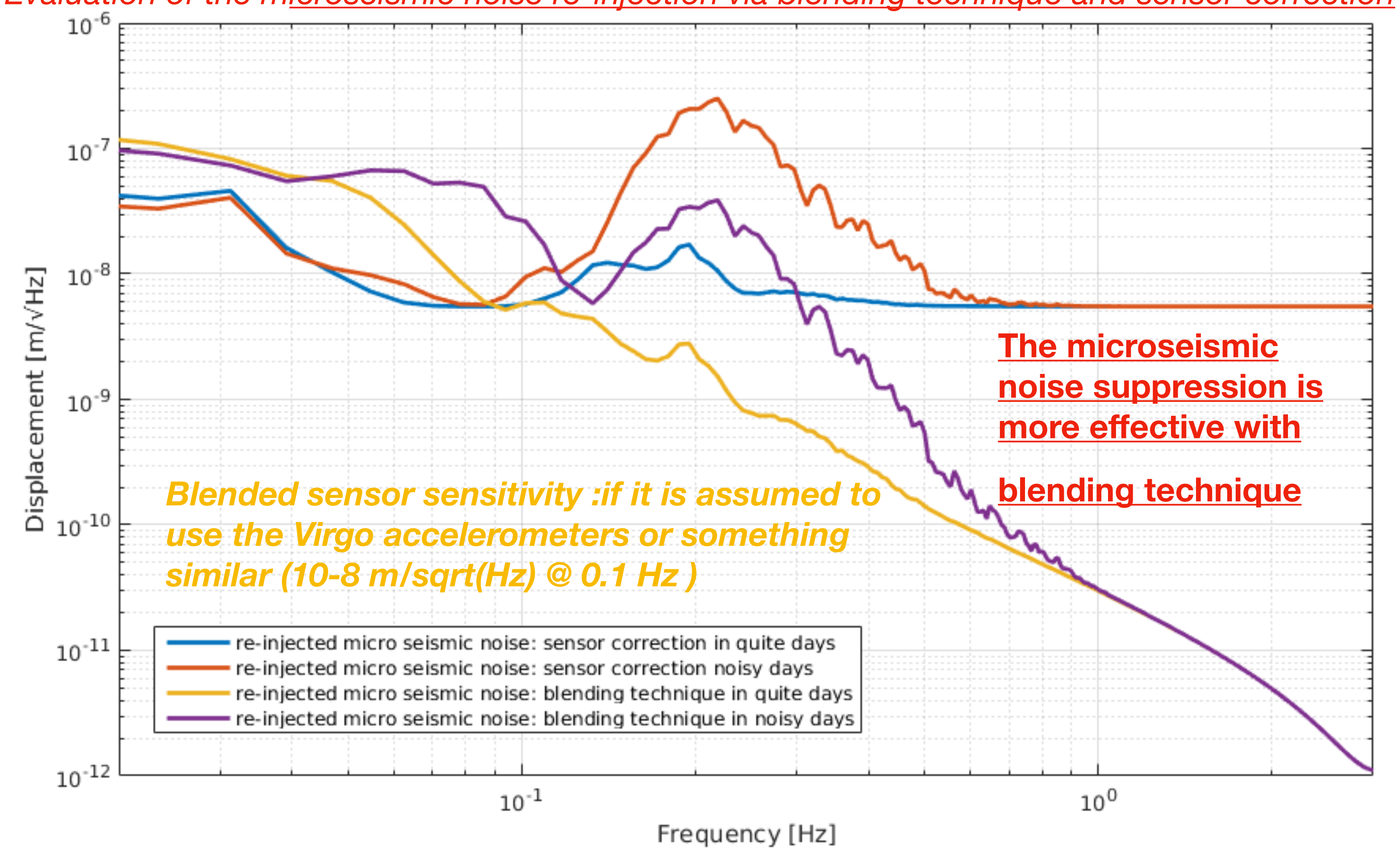

The noise of the KAGRA inertial sensor is re-injected via loop causing the grow in up of the peak @ 0.148 Hz: this means that the loop is exciting the test mass at that frequency and is hard to lock the ITF (more details see following klogs):

http://klog.icrr.u-tokyo.ac.jp/osl/?r=7395

http://klog.icrr.u-tokyo.ac.jp/osl/?r=7447

http://klog.icrr.u-tokyo.ac.jp/osl/?r=9981

http://klog.icrr.u-tokyo.ac.jp/osl/?r=10228

http://klog.icrr.u-tokyo.ac.jp/osl/?r=10187

http://klog.icrr.u-tokyo.ac.jp/osl/?r=9995

http://klog.icrr.u-tokyo.ac.jp/osl/?r=8571

http://klog.icrr.u-tokyo.ac.jp/osl/?r=8567

Sensor Correction (SC)

- **Sensor correction**

The virtual sensor is attained through the subtraction of the seismic noise (measured by seismometer) and the LVDT signal

$$S(\omega) = S_{LVDT}(\omega) - HP_{SC}(\omega) \cdot S_{seim}(\omega)$$

Typical shape TF from ground to LVDT

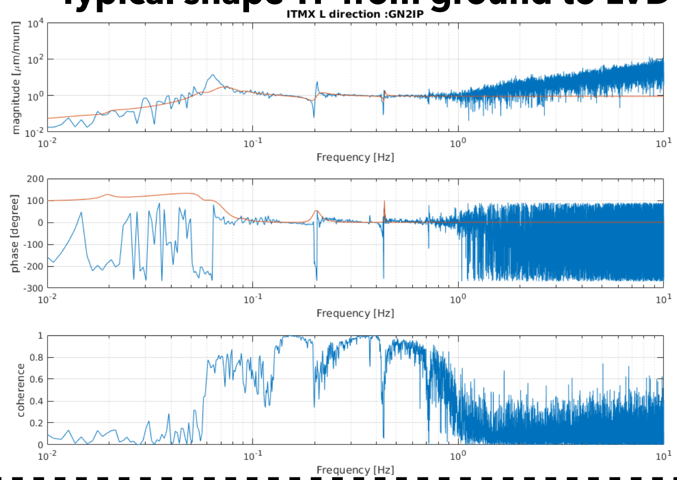

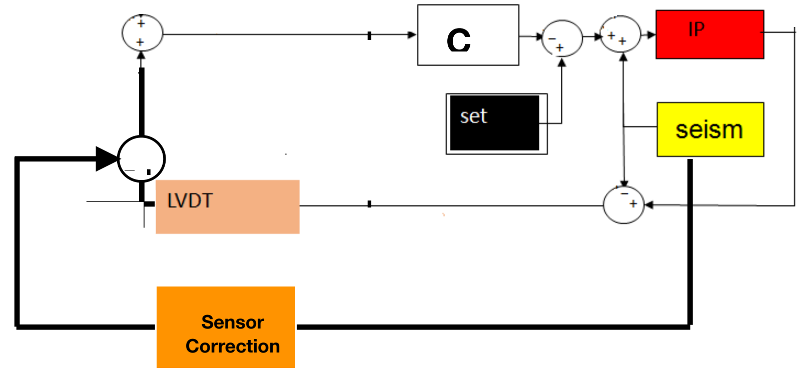

Typical shape HP filter

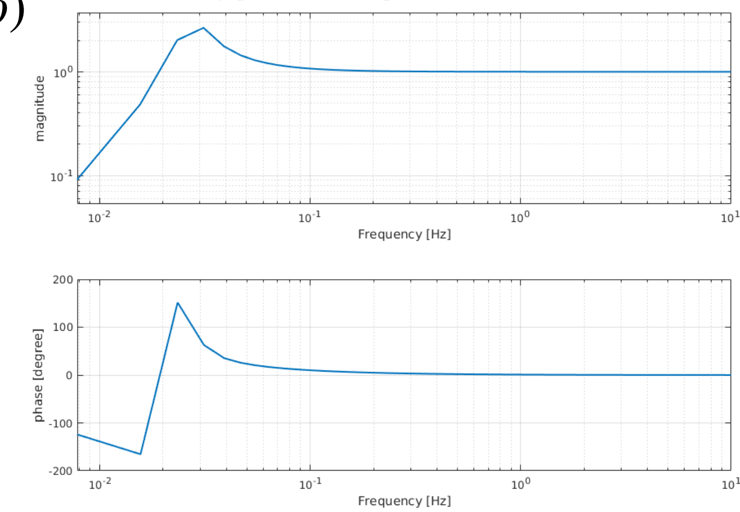

IP L

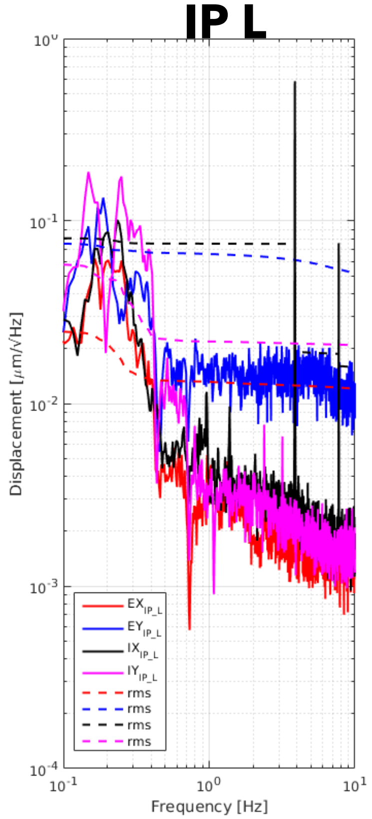

IP T

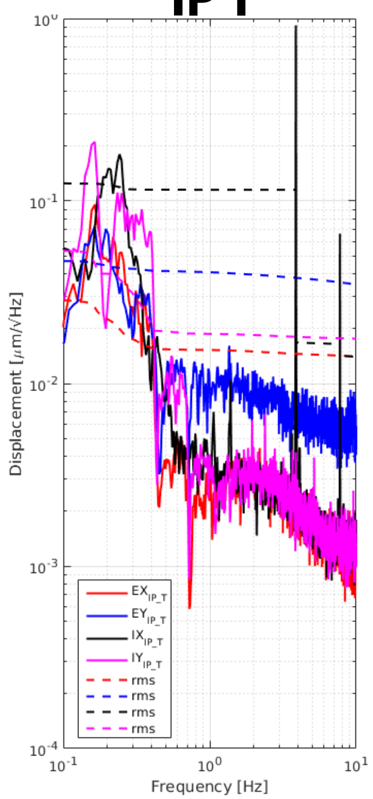

IP Y

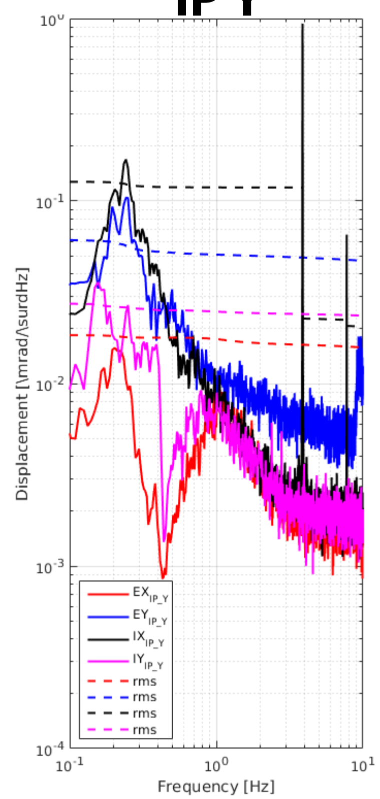

RMS	L[μm]	T [μm]	Y[μrad]
IX	0.08	0.09	0.09
EX	0.06	0.06	0.08
IY	0.08	0.07	0.08
EY	0.07	0.07	0.08

Thanks to sensor correction technique, the rms of IP motion is suppressed by a factor 3 (*http://klog.icrr.u-tokyo.ac.jp/osl/?r=13452*)

Type A: SC noise budget (I)

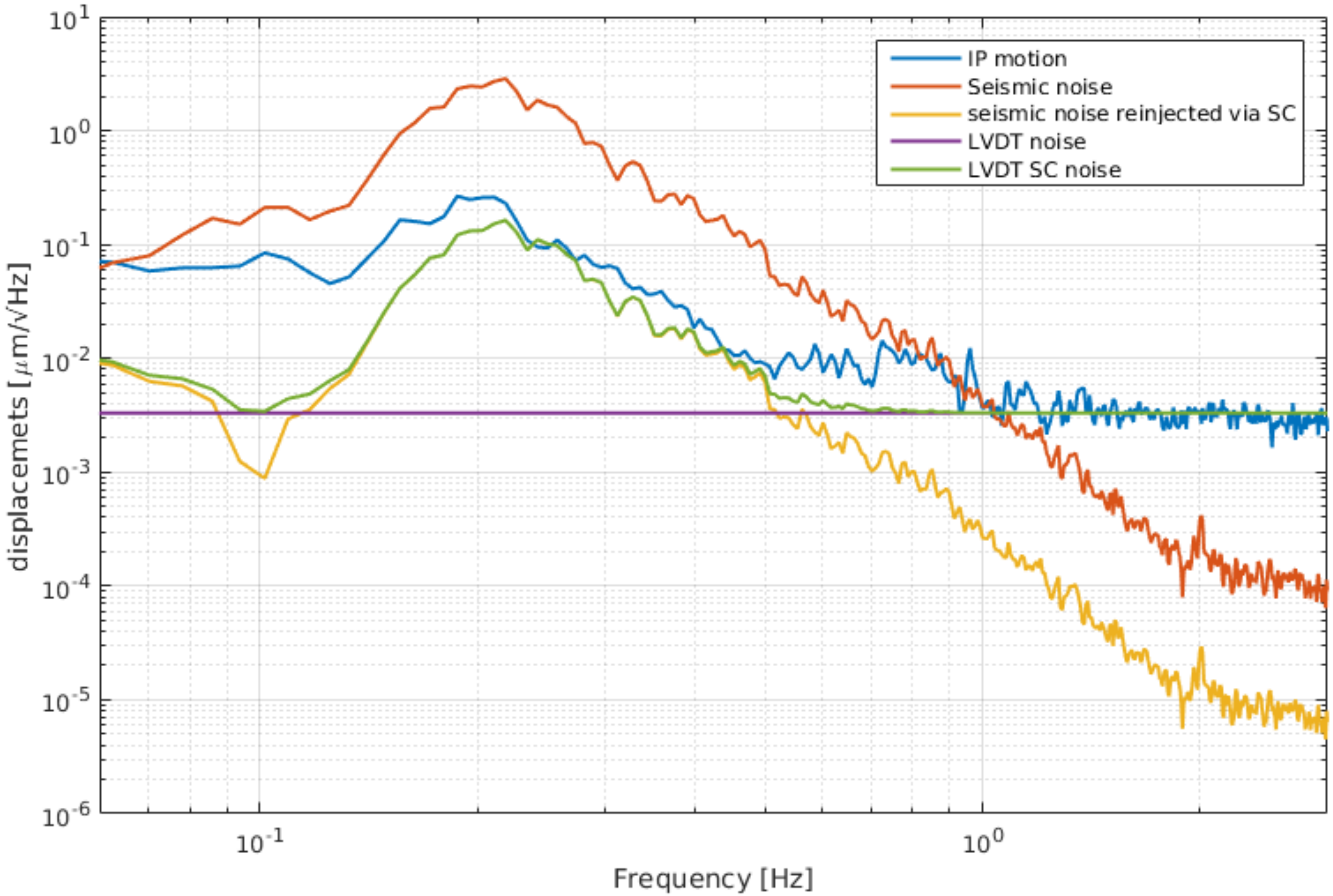

The seismic noise @ 0.150 Hz is suppressed, but the IP motion is still limited by it.

Above 1 Hz the IP motion is limitedly the LVDT noise

Type A: SC noise budget (II)

Let's consider now the SC performance in the following seismic noise conditions

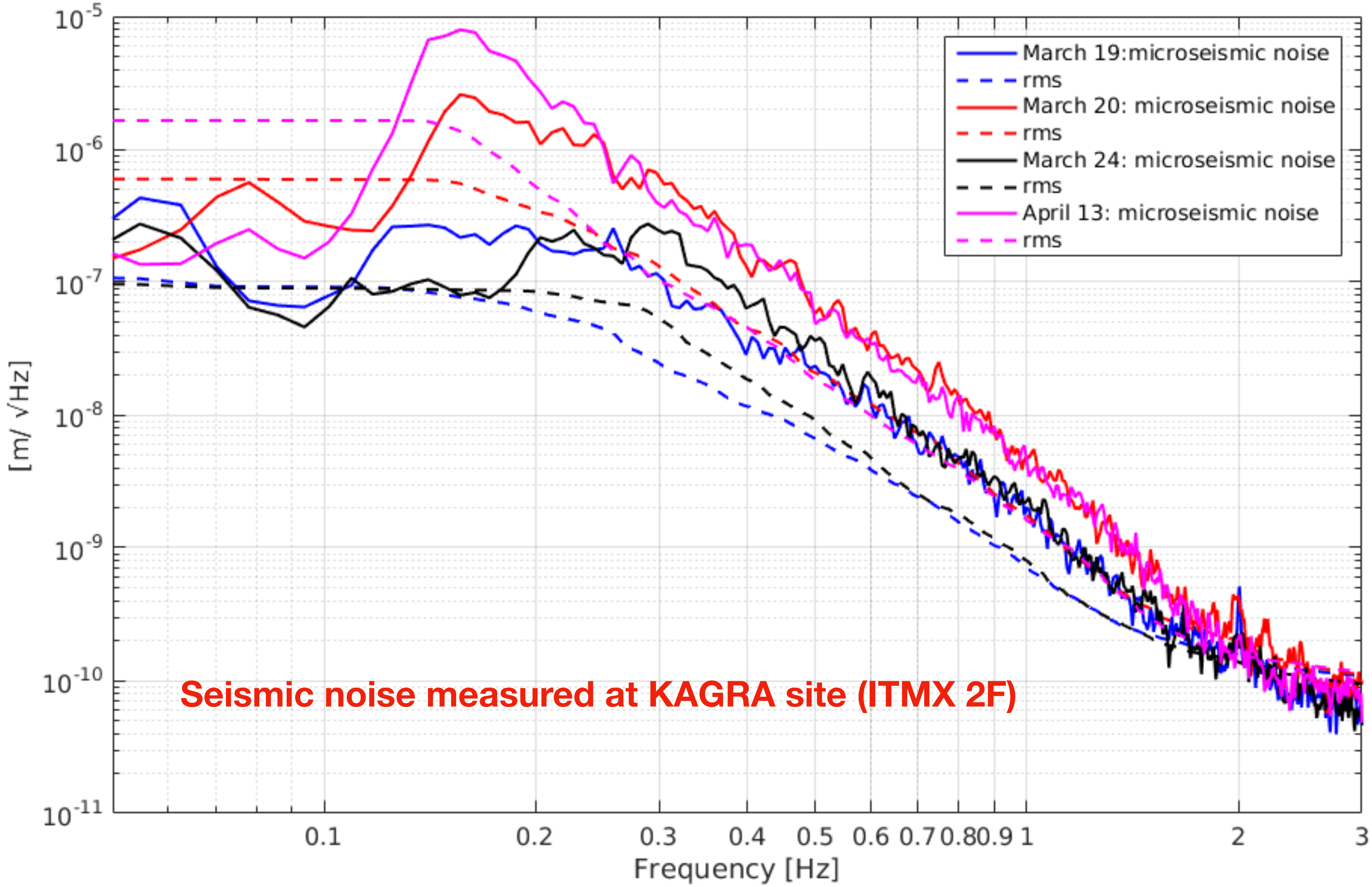

Type A: SC noise budget (III)

The plot shows how the IPs spectra along L direction is changing in relation to the micro-seismic noise variation.

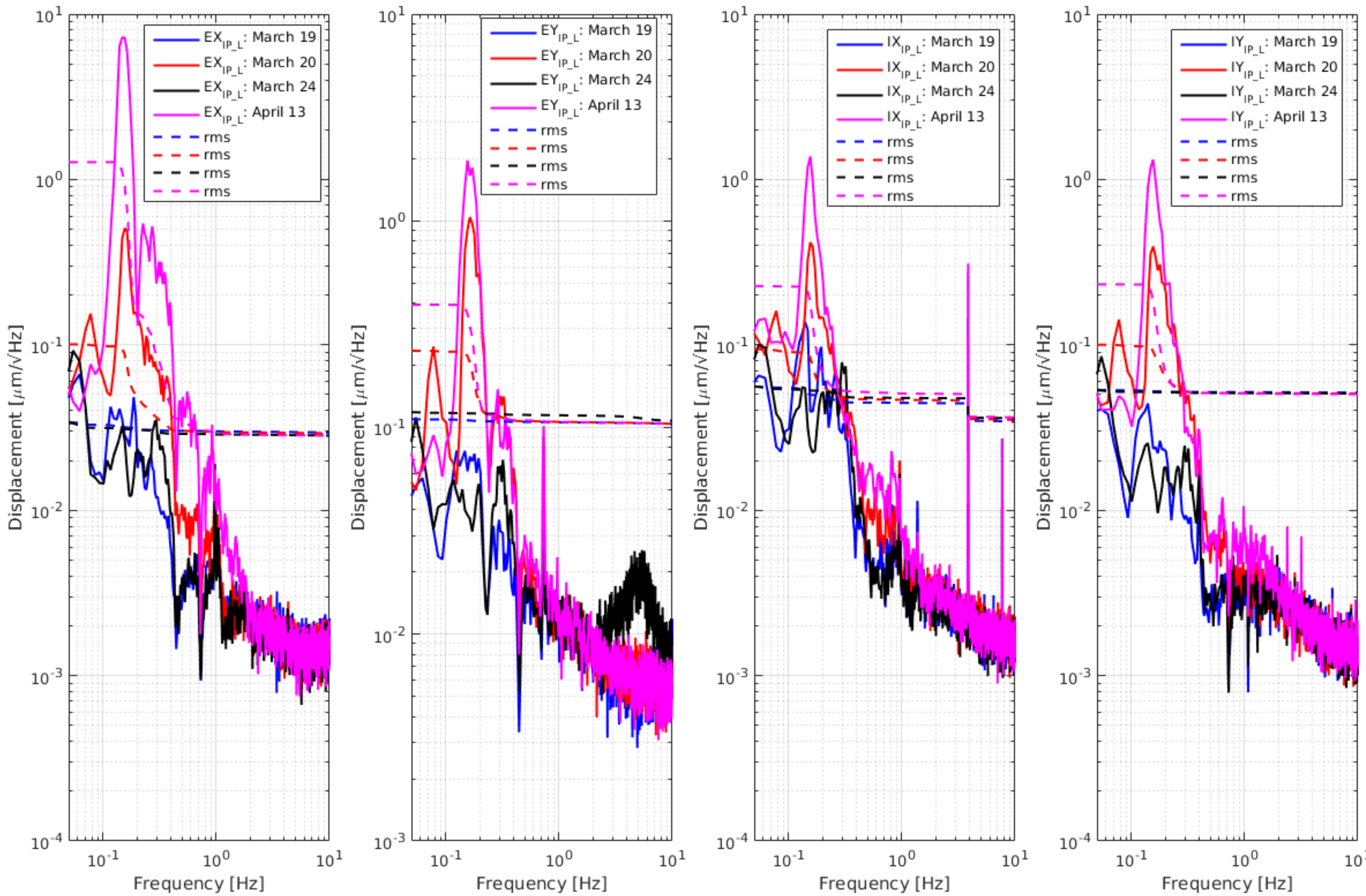

In noisy days the IP rms is got worse more then a factor 8 (IX, IY, EY)

In noisy days the IP rms is got worse more then a factor 10 (EX)

Type A: SC noise budget (VII)

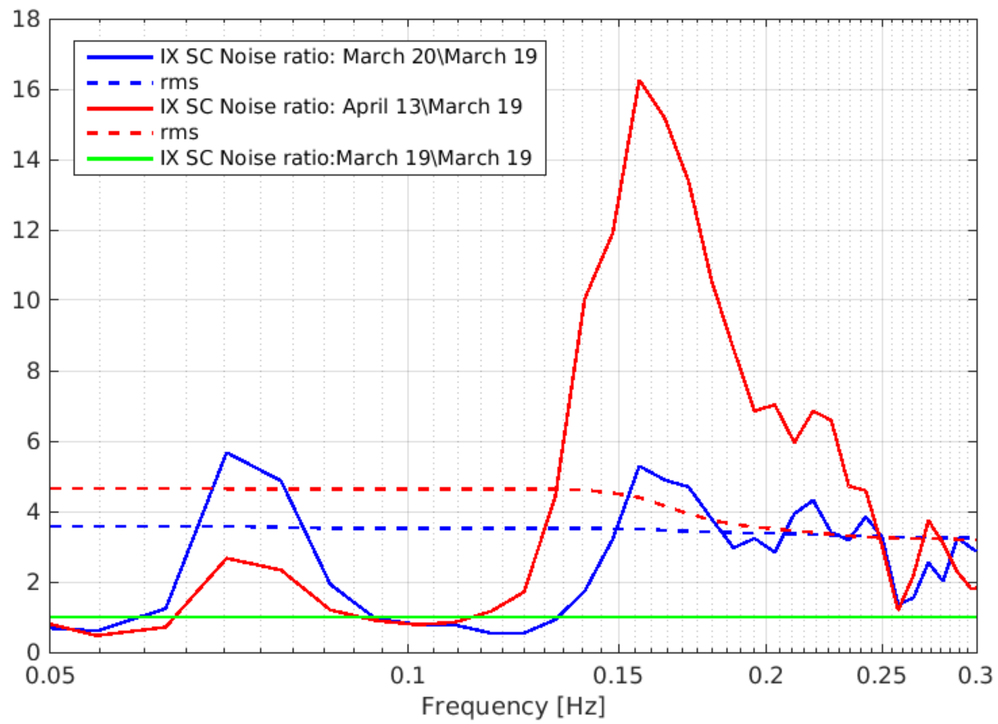

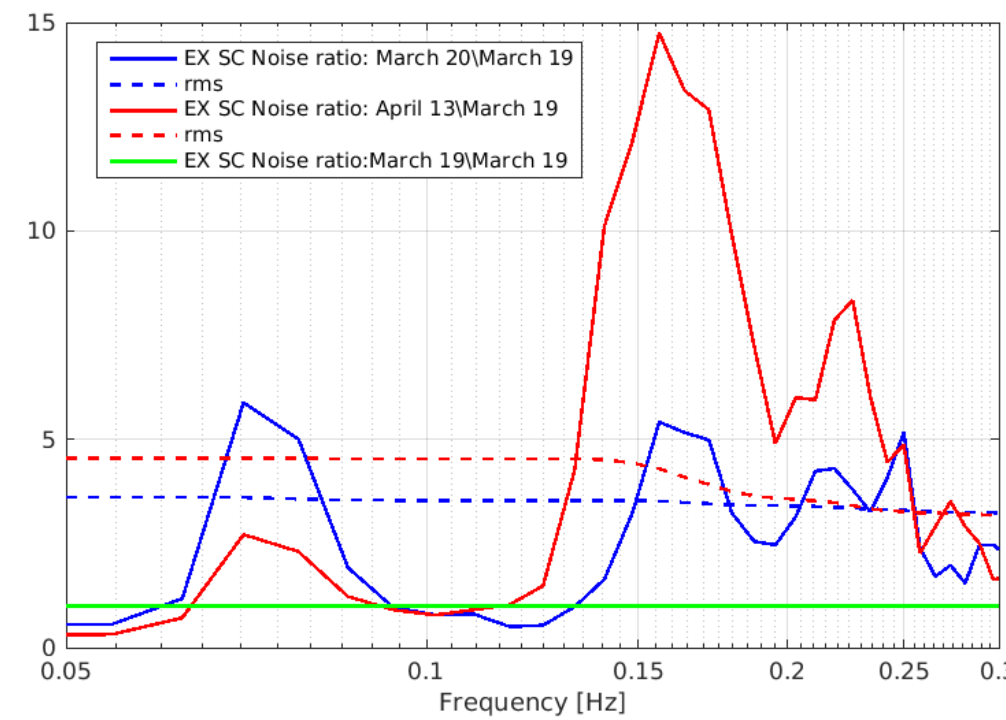

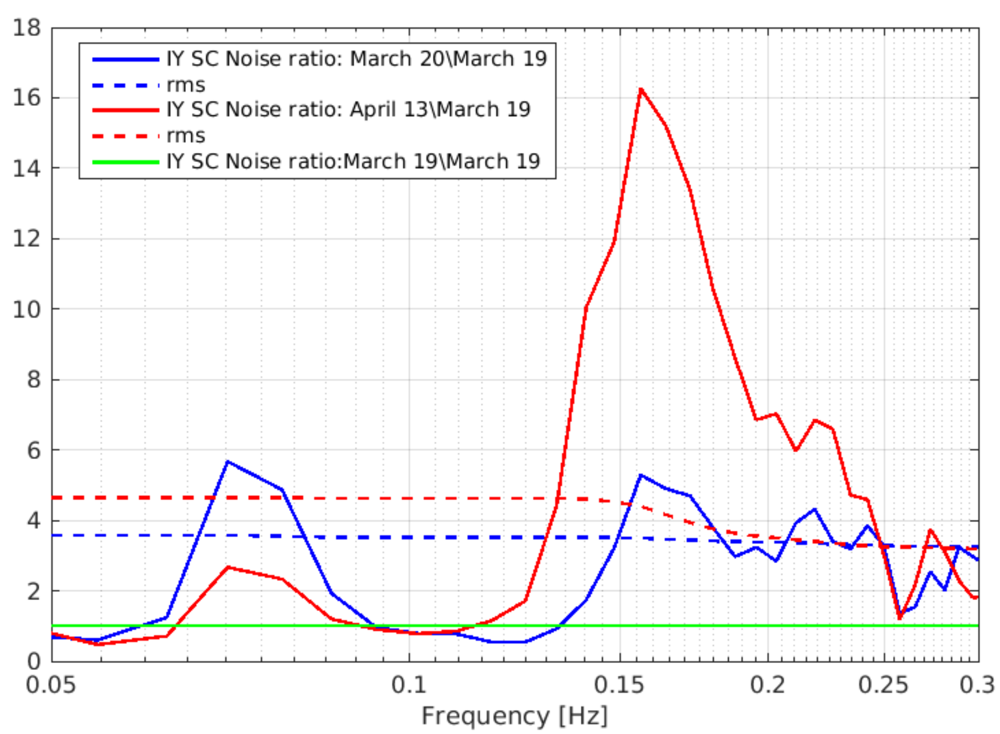

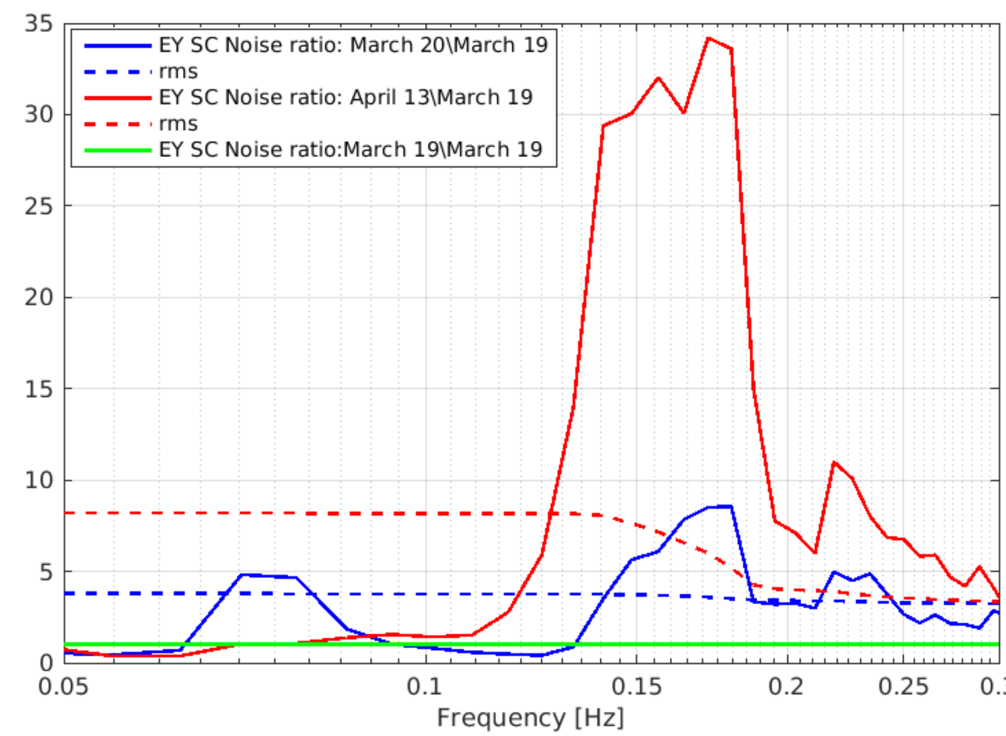

In noisy days (like March 20) the rms of the seismic re-injection is got worse by a factor 3.4

In noisy days (like April 13) the rms of the seismic re-injection is got worse by a factor 5 at IX,IY,EX and a factor 7.5 at EY

Type A GAS filter: EY case

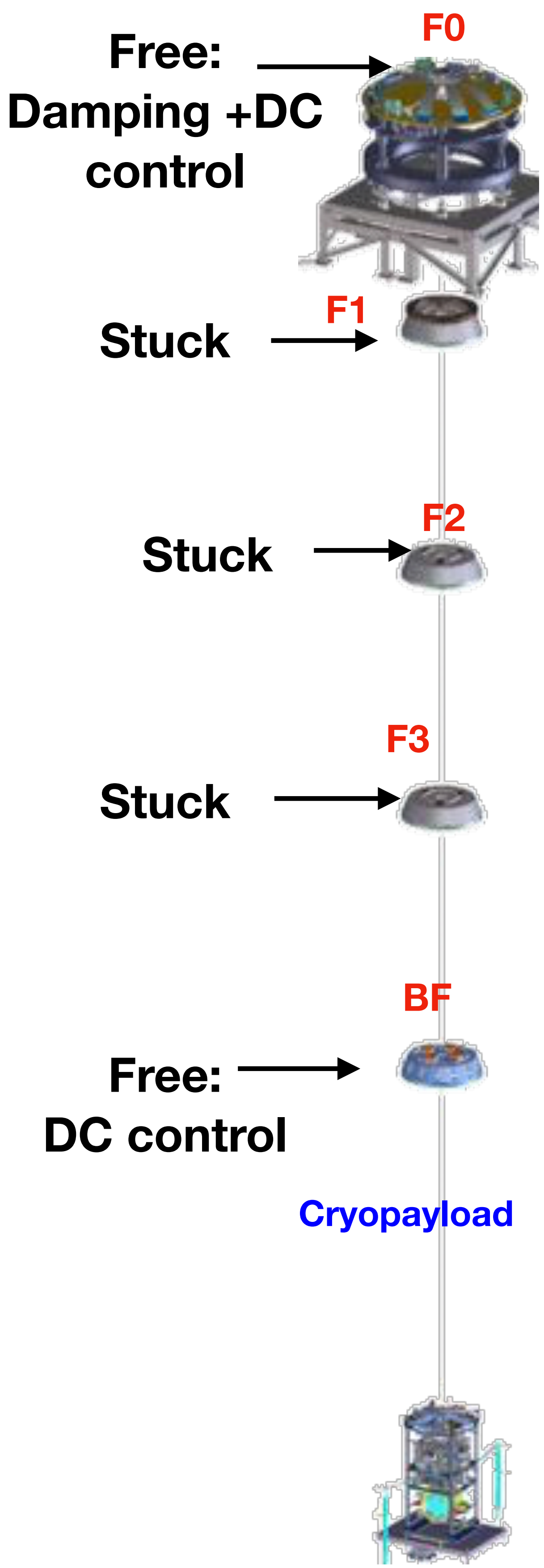

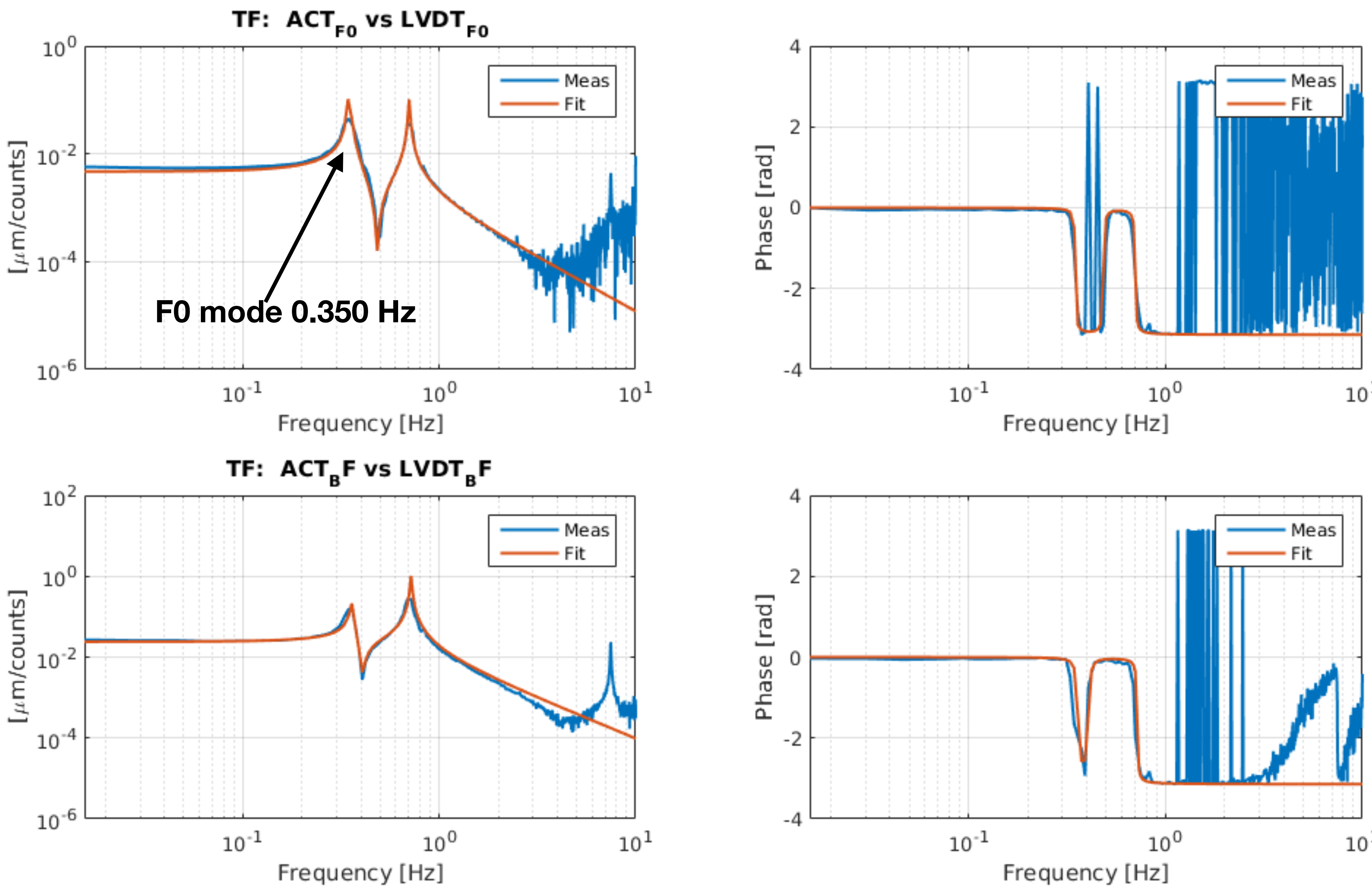

Three stages missing

The TF from F0 to TM loses $\frac{1}{f^6}$ in terms of mechanical attenuation

Vertical seismic noise re-injected via F0 to TM has to be evaluated

F0 GAS filter: noise budget (I)

Feedback control scheme

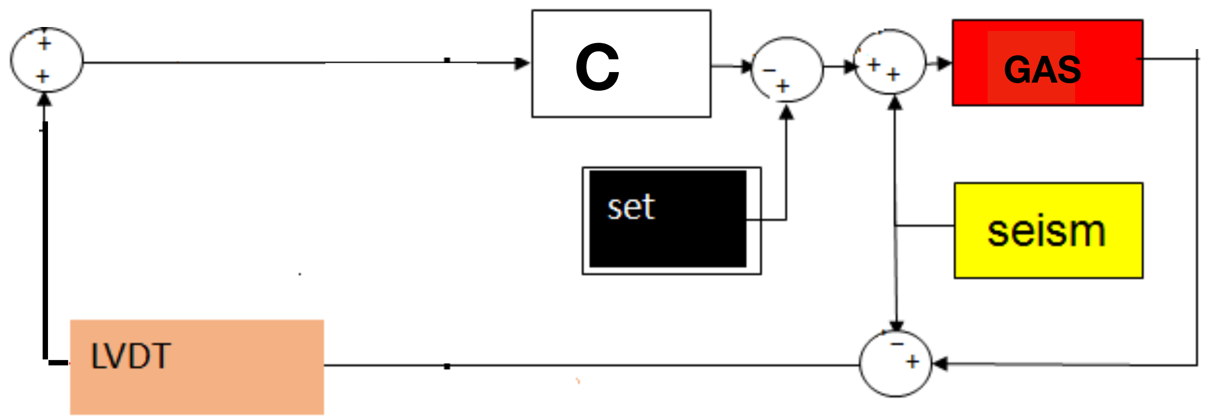

GAS filter= mechanical system

LVDT= is the sensor monitoring the displacement

$$x_{lvdt} = x_{F0} - x_0$$

x_0 **is the ground motion**

set= is the set point

C= is the damping filter

In this configuration:

GAS filter LVDT signal = Error signal

$$\tilde{S}_{iv}^{CL}(\omega) = \frac{\tilde{S}_{iv}(\omega)}{1 - \tilde{M}_i(\omega) \cdot \tilde{C}_i(\omega)}$$

In this configuration two sources of noise can be identified:

- **LVDT noise (I)**
- **Seismic noise (S)**

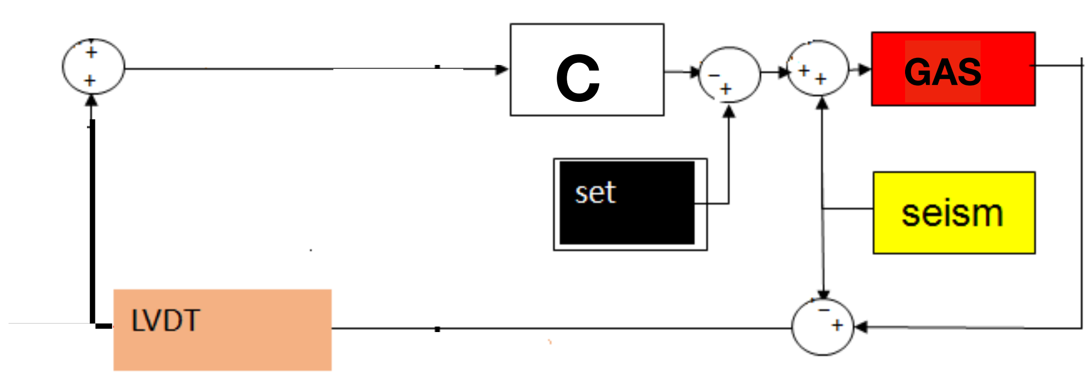

Let's assume that these noise are:

$$S_{noise} = \sqrt{I^2 + S^2}$$

F0 GAS filter: noise budget (II)

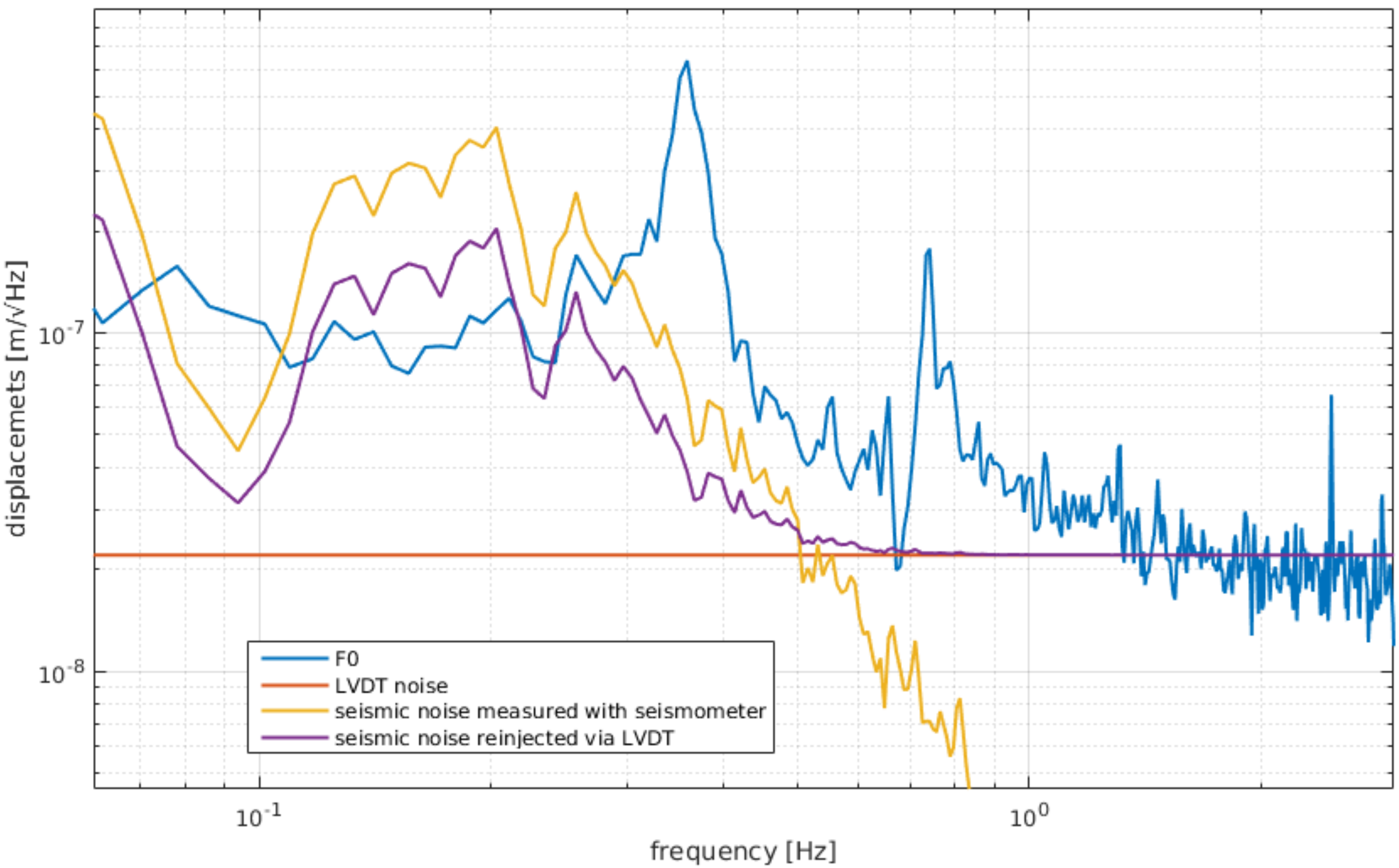

Below 0.3 Hz the F0 motion is limited by seismic noise

Above 1 Hz the F0 motion is limited by the LVDT noise

F0 GAS filter: noise budget (III)

Let's consider now the F0 performance in the following seismic noise conditions

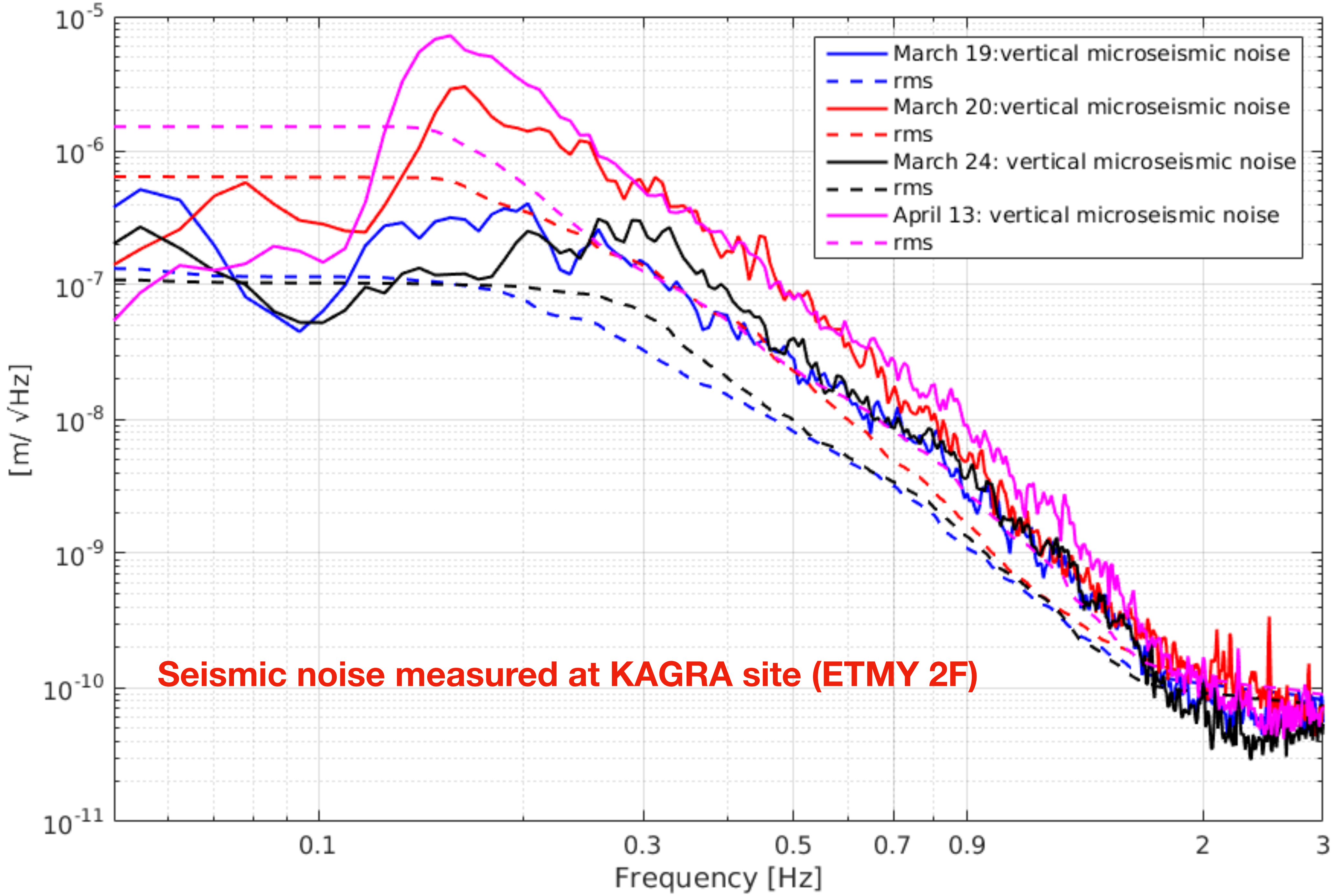

F0 GAS filter: noise budget (IV)

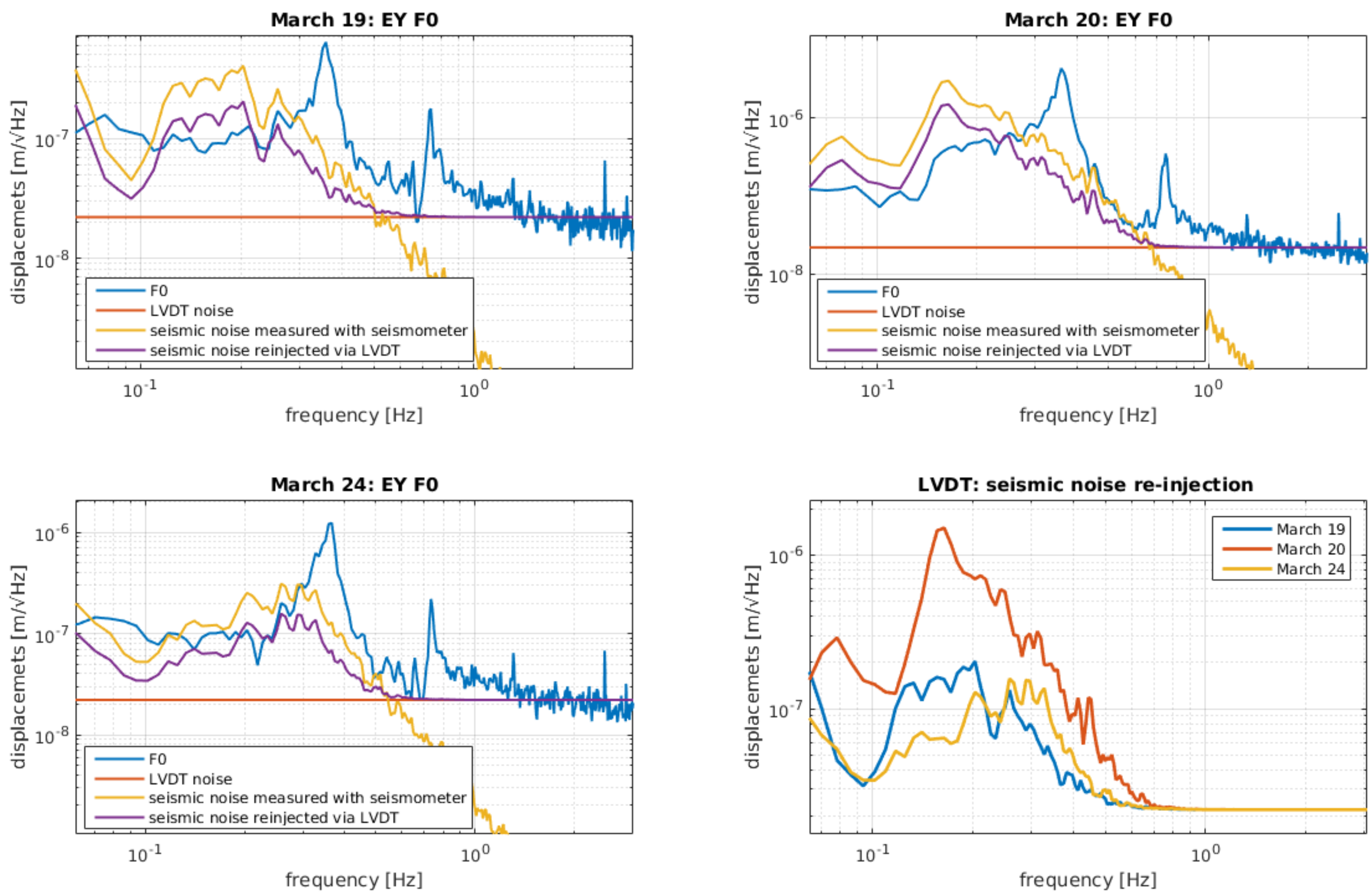

Below 0.3 Hz the F0 motion is limited by seismic noise

In noisy days the seismic re-injection is got worse by a factor 6

KAGRA low frequency sensitivity (I)

KAGRA's detection band is [10 Hz, 10 kHz]

Below 10 Hz the KAGRA sensitivity is limited by mechanical noise:

- **Horizontal Seismic noise where the mechanical attenuation is low f<2 Hz**

- **Vertical Seismic noise transmitted to the horizontal direction due to the inclination of the test mass**

- **Angular control noise f<10 Hz**

- **Other possible control or actuation noise**

Let's focus on the first two noise sources…

KAGRA low frequency sensitivity (II)

The strain sensitivity is defined as following: $h(t) = \frac{\Delta L}{L}$

Where ΔL is the differential length variation $\Delta L = D_{arm} = X_{arm} - Y_{arm}$

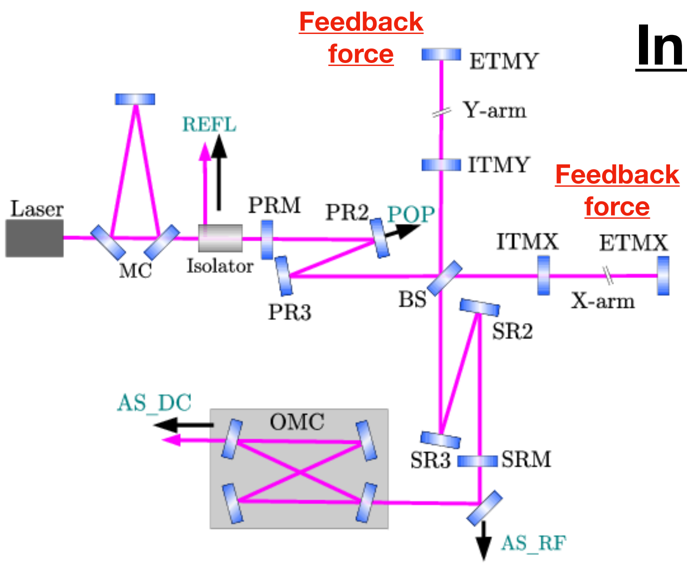

In KAGRA interferometer the detection band is [10 Hz, 10 kHz]

What about the KAGRA sensitivity below 10 Hz??

*One way to deduce it is to use the feedback force (**F**) sent through the End TMs filtered with the transfer function **M** (actuation-displacement along the optical axis of the mirror).*

$$\Delta L_{LF}(\omega) = \sqrt{(F_{EX} \cdot M_{EX})^2 + (F_{EY} \cdot M_{EY})^2}$$

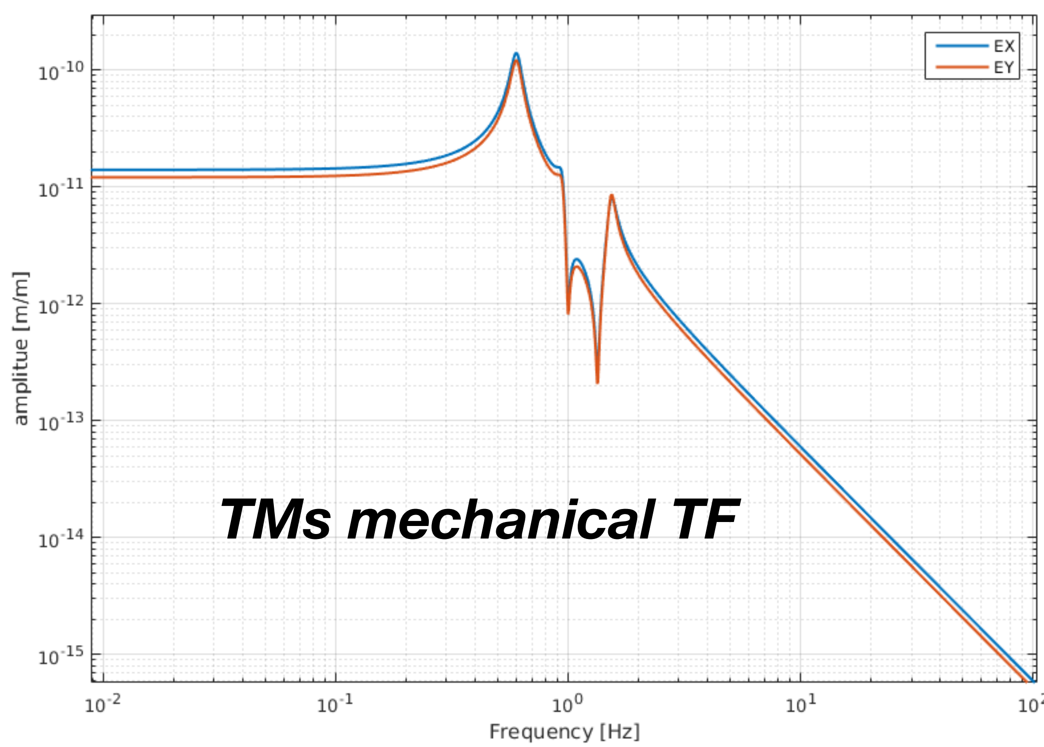

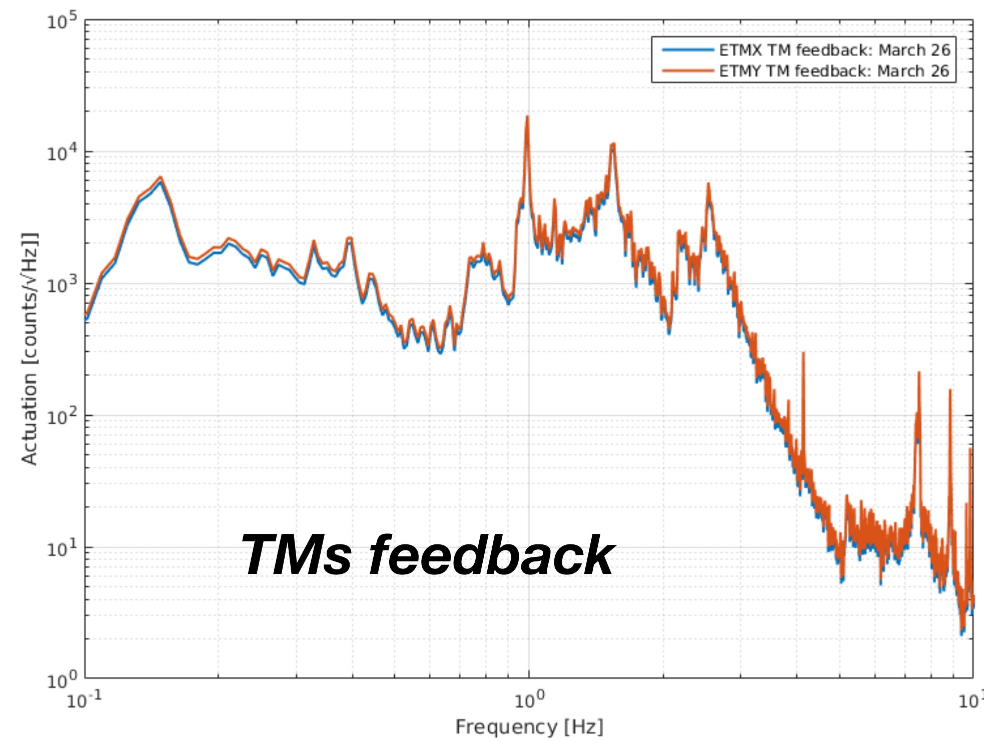

KAGRA low frequency sensitivity (III)

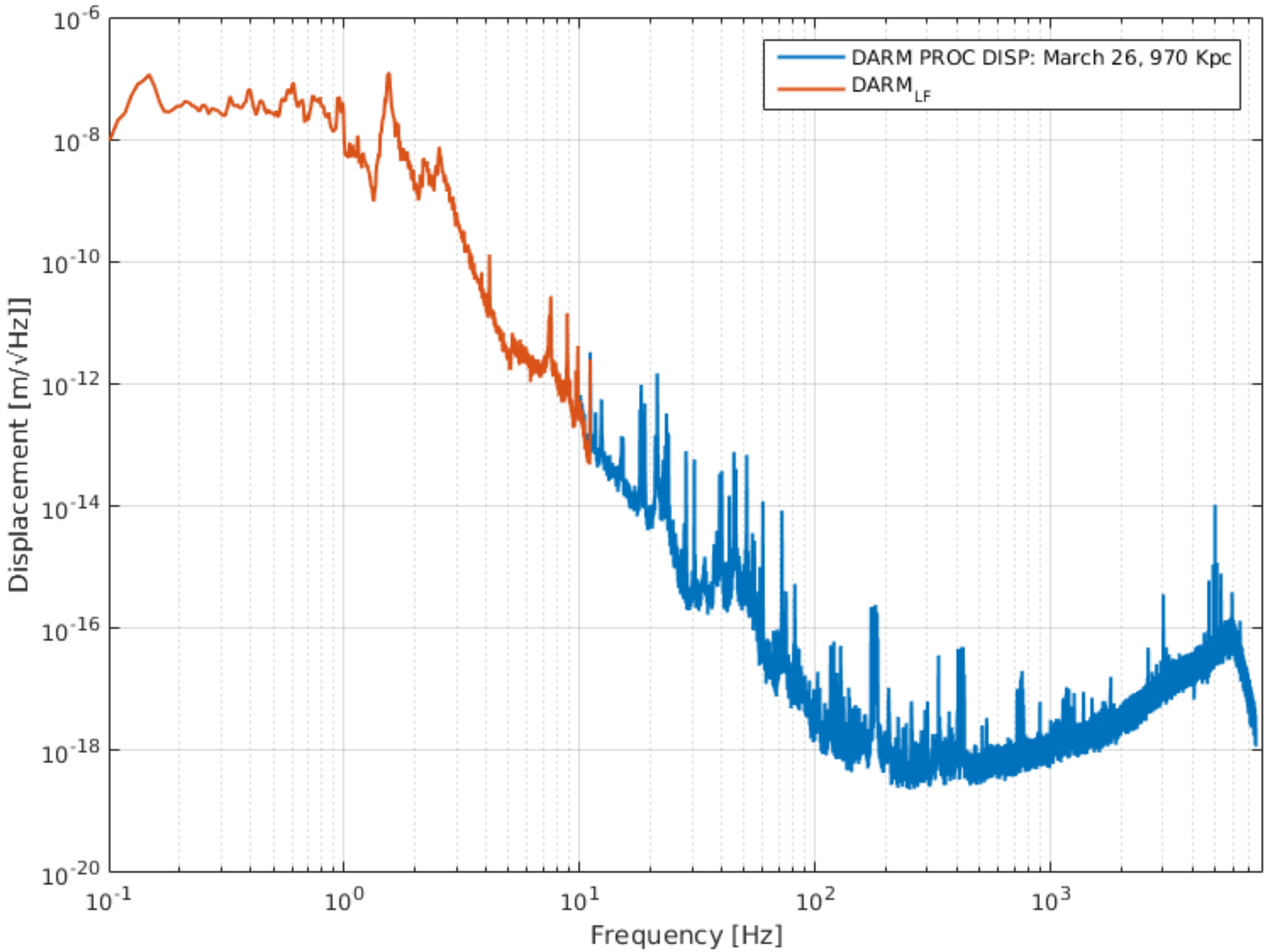

@ 10 Hz the curves are matching

KAGRA low frequency sensitivity: Type A mechanical noise (I)

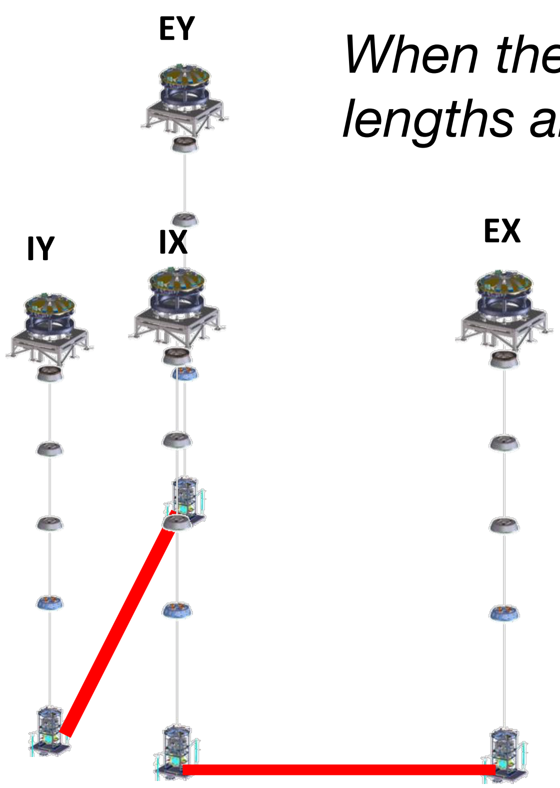

When the interferometer works in dark fringe condition, in first approximation, the cavity lengths are fixed through the locking of the four TMs.

*Below 2 Hz, where the Type A mechanical attenuation is low and the SC acts, the IP residual motion is transmitted to TM filtered with the transfer function ****D*** *(displacement-displacement IP to TM along the optical axis of the mirror):*

$$S_{TM} = S_{IP} \cdot D_{IP2TM}$$

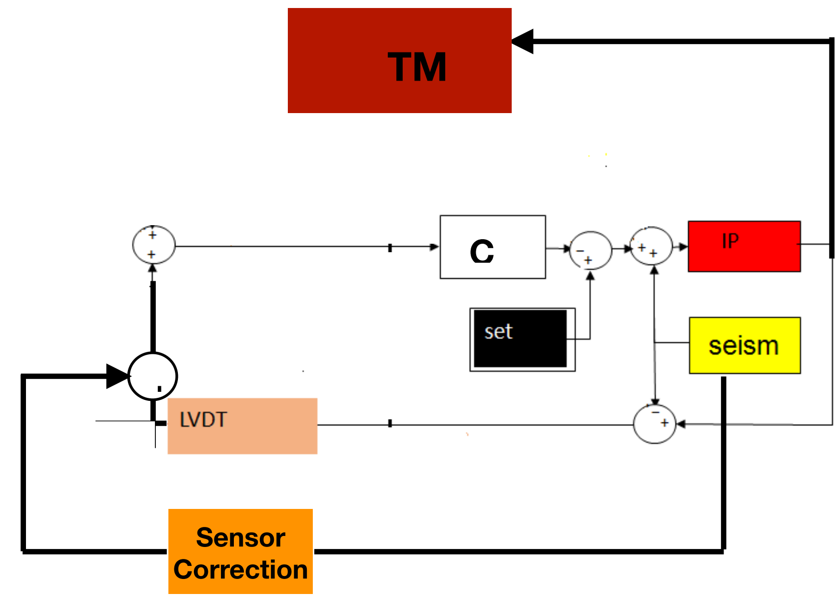

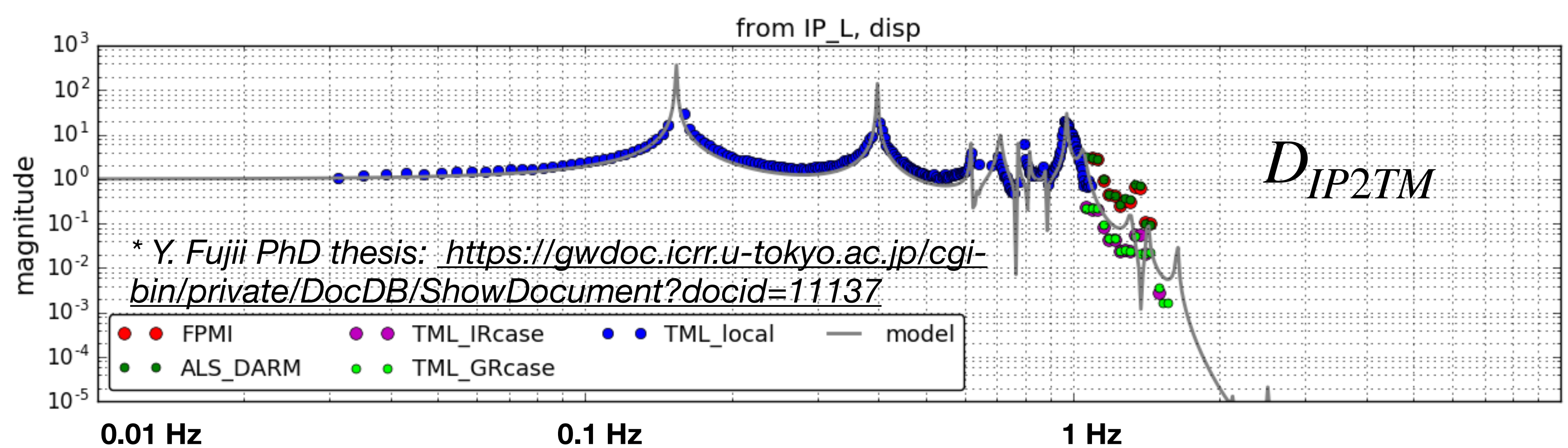

** Y. Fujii PhD thesis: https://gwdoc.icrr.u-tokyo.ac.jp/cgi-bin/private/DocDB/ShowDocument?docid=11137*

By combining the IP signals of the four Type A It is possible to estimate the contributions of the longitudinal mechanical noise onto the sensitivity as following:

$$\Delta L_{IP}(\omega) = \sqrt{(IP_{EX} \cdot D_{IP2TM})^2 + (IP_{IX} \cdot D_{IP2TM})^2 + (IP_{EY} \cdot D_{IP2TM})^2 + (IP_{IP2TM} \cdot D_{IP2TM})^2}$$

KAGRA low frequency sensitivity: Type A mechanical noise (II)

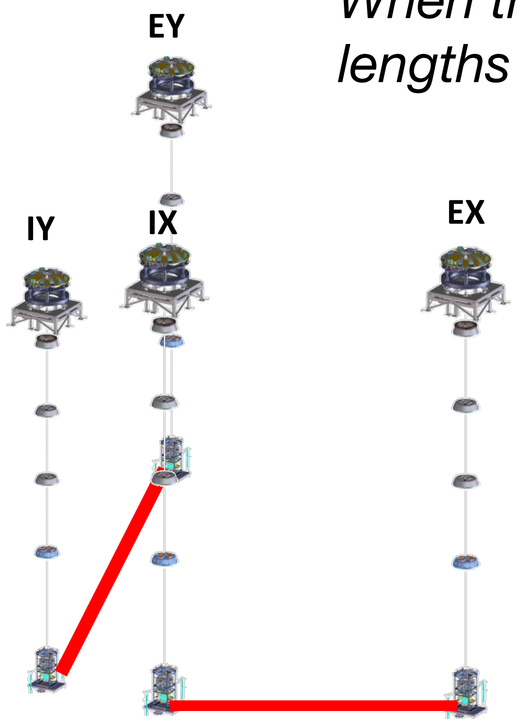

When the interferometer works in dark fringe condition, in first approximation, the cavity lengths are fixed through the locking of the four TMs.

Due to Earth curvature, a vertical to horizontal coupling is expected and for this reason It is interesting to estimate the impact of the EY vertical residual motion onto the sensitivity curve.

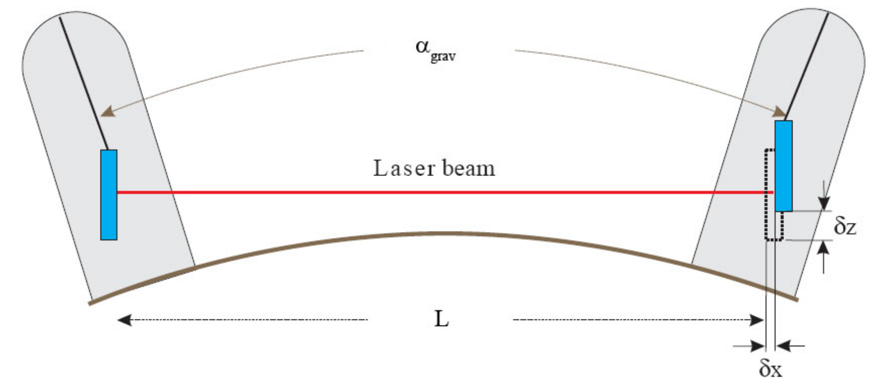

*Below 2 Hz, where the Type A mechanical attenuation is low F0 residual motion is transmitted to TM filtered with the transfer function ****D1:***

$$S_{TM} = \alpha_{grav} \cdot D_1 \cdot S_{F0}$$

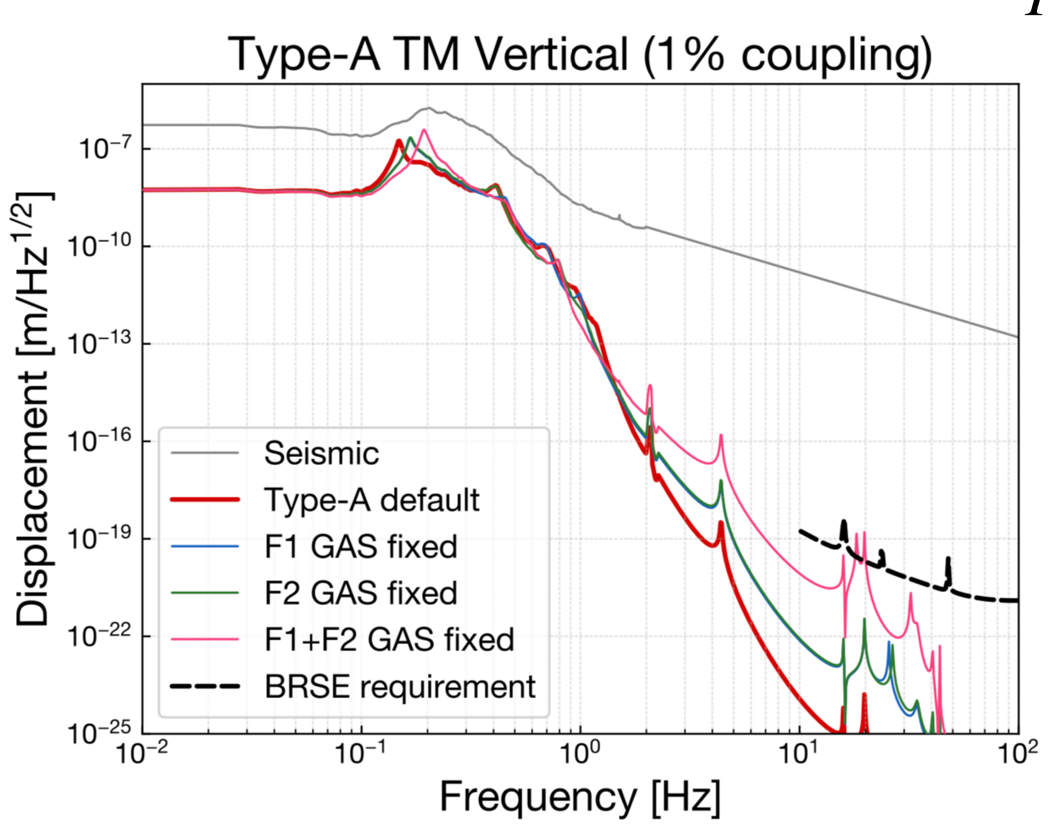

Theoretical D1 in different configuration:
-Default (all GAS filters working properly)
-1 GAS filters stuck
-2 GAS filter stuck:@ 10 Hz the attenuation is about 10^-19

* *K.Okutomi: https://gwdoc.icrr.u-tokyo.ac.jp/DocDB/0081/G1808125/002/TypeAfixedGAS20180403v2.pdf*

What about 3 GAS filters stuck?

KAGRA low frequency sensitivity: Type A mechanical noise (II)

Due to Earth curvature, a vertical to horizontal coupling is expected and for this reason It is interesting to estimate the impact of the EY vertical residual motion onto the sensitivity curve.

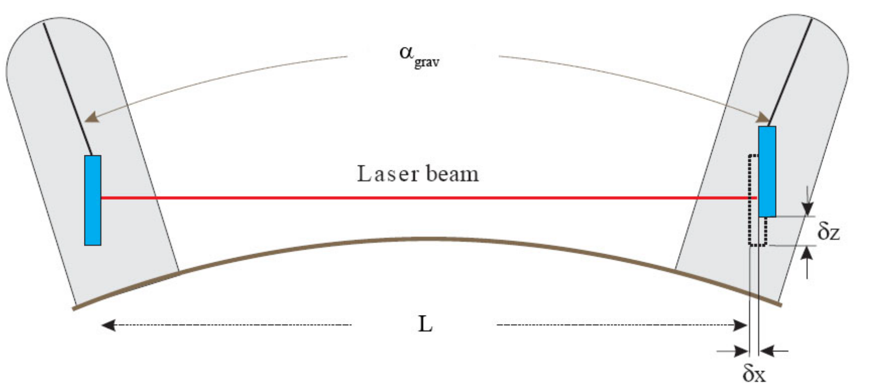

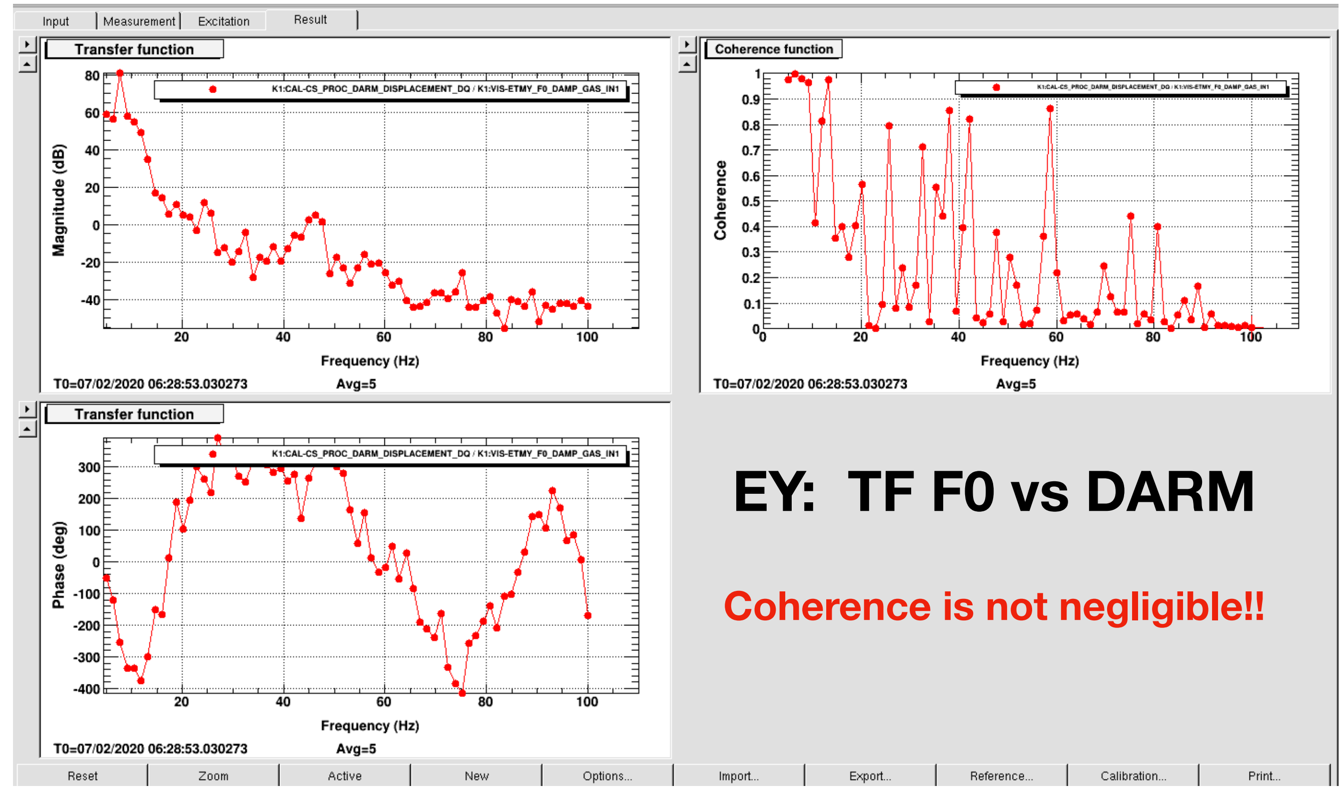

EY: calibrated TF F0 vs DARM

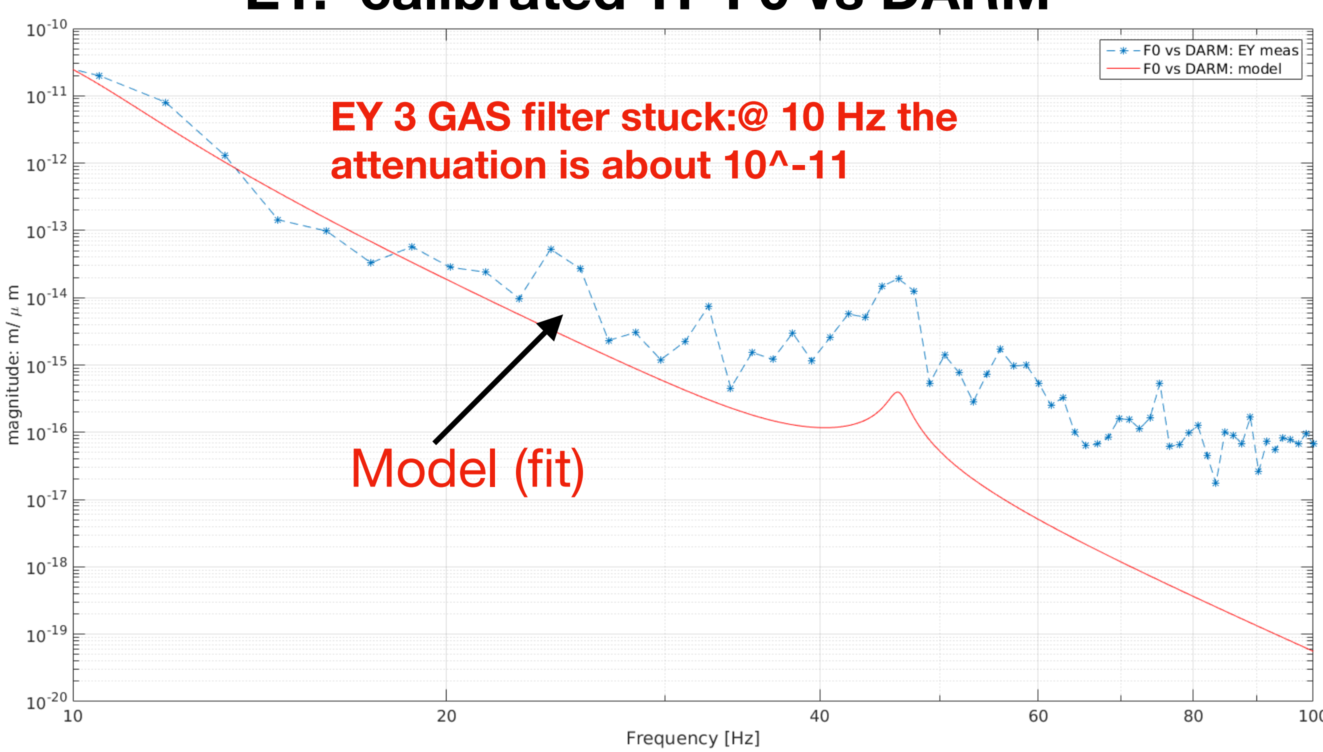

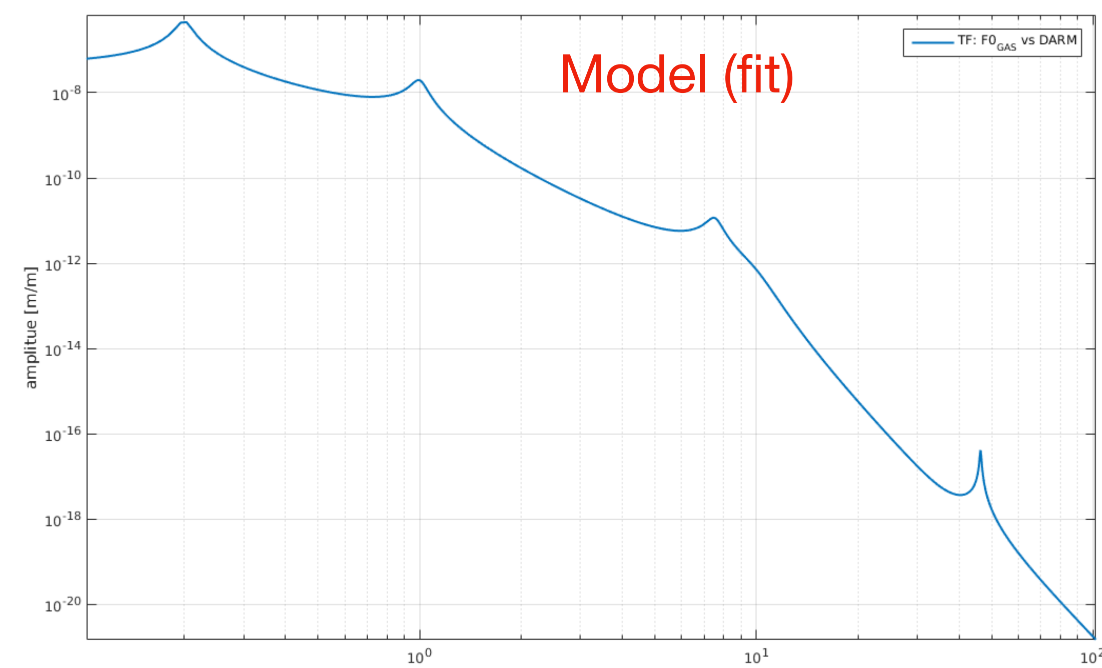

<u>Could limiting the sensitivity</u>

KAGRA low frequency sensitivity: Type A mechanical noise (III)

By combining the Type A IP signals and EY F0 (filtered with the mechanical TFs) It is possible to project their mechanical noise contribution onto the DARM sensitivity.

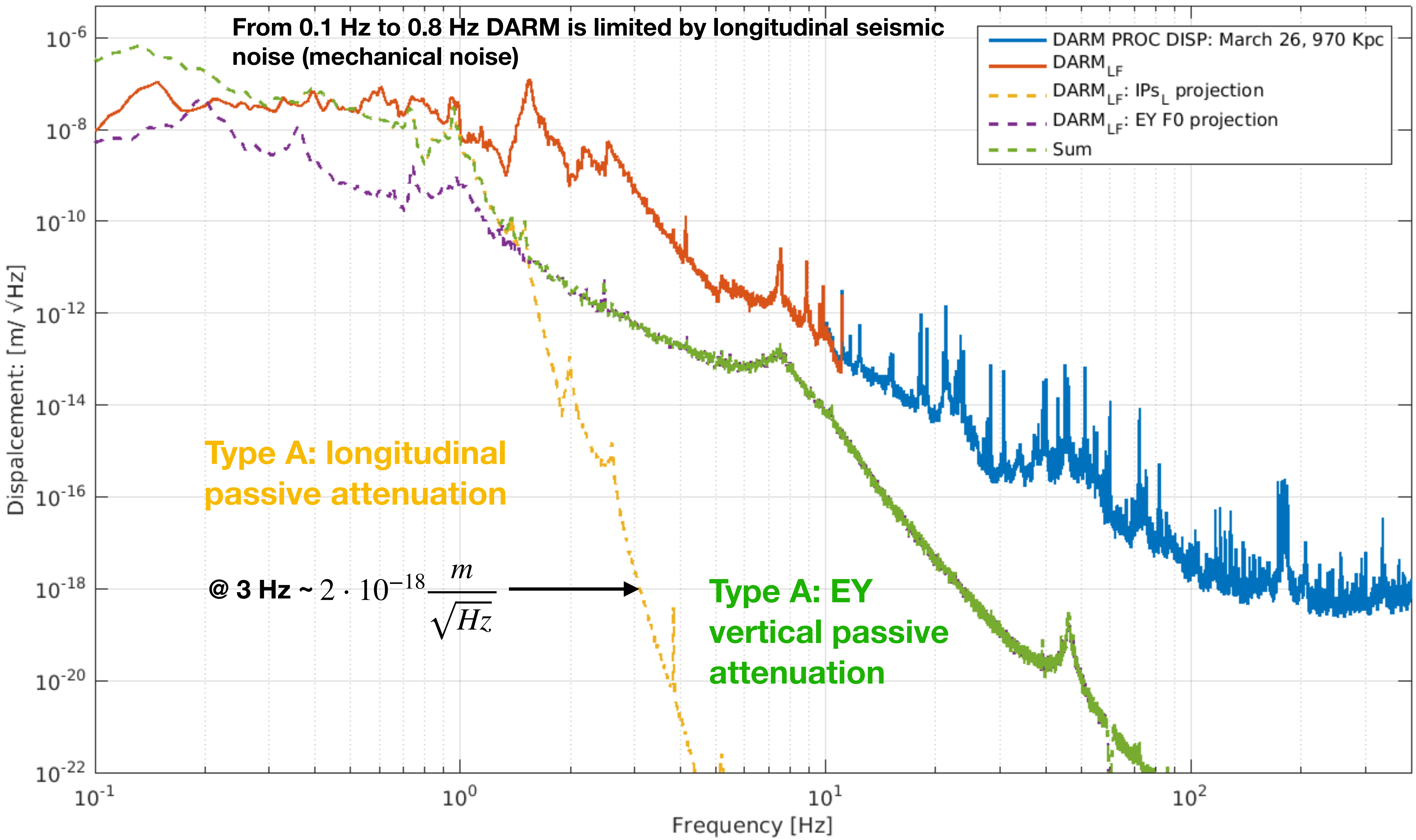

KAGRA low frequency sensitivity: Type A performance (I)

Let's consider now the type A performance in the following seismic noise conditions

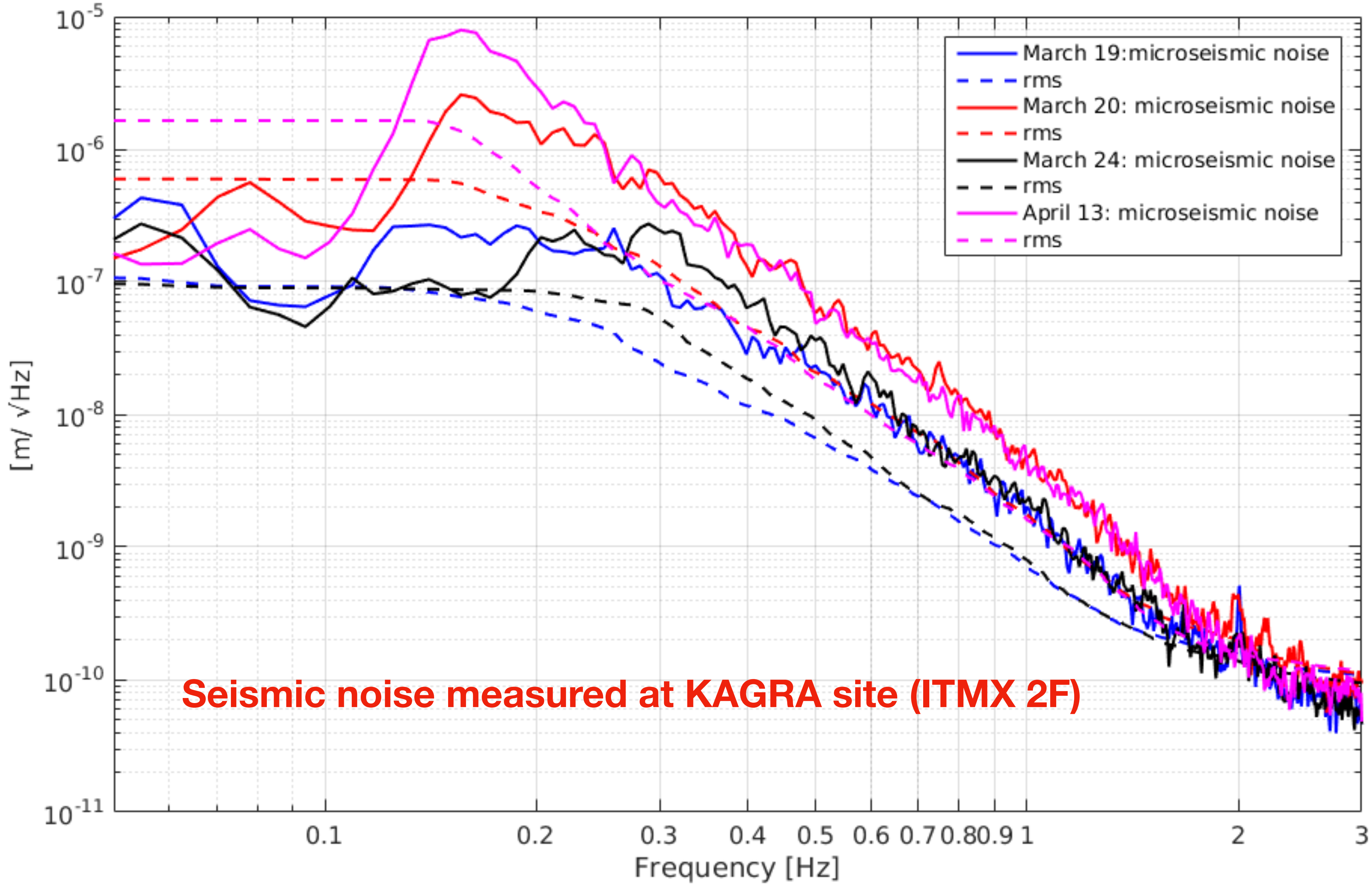

IFO locked: March 19, March 20, March 24

Due to the huge microseismic noise the IFO couldn't be locked: April 13

KAGRA low frequency sensitivity: Type A performance (II)

The plot shows how the IPs spectra along L direction is changing in relation to the micro-seismic noise variation.

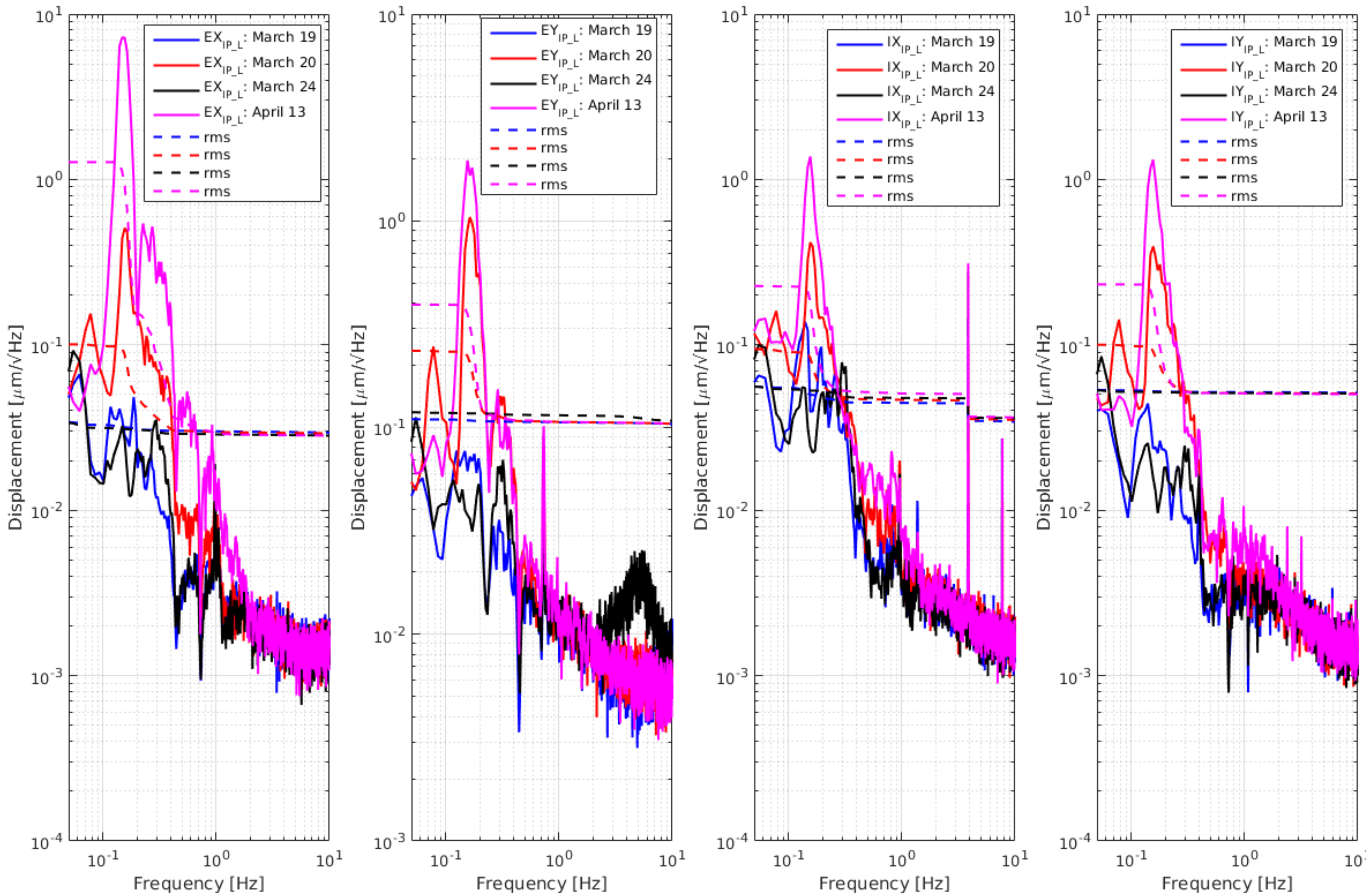

In noisy days the IP rms is got worse more then a factor 8 (IX, IY, EY)

In noisy days the IP rms is got worse more then a factor 10 (EX)

KAGRA low frequency sensitivity: Type A performance (III)

The plot shows how the EY F0 spectra is changing in relation to the micro-seismic noise variation.

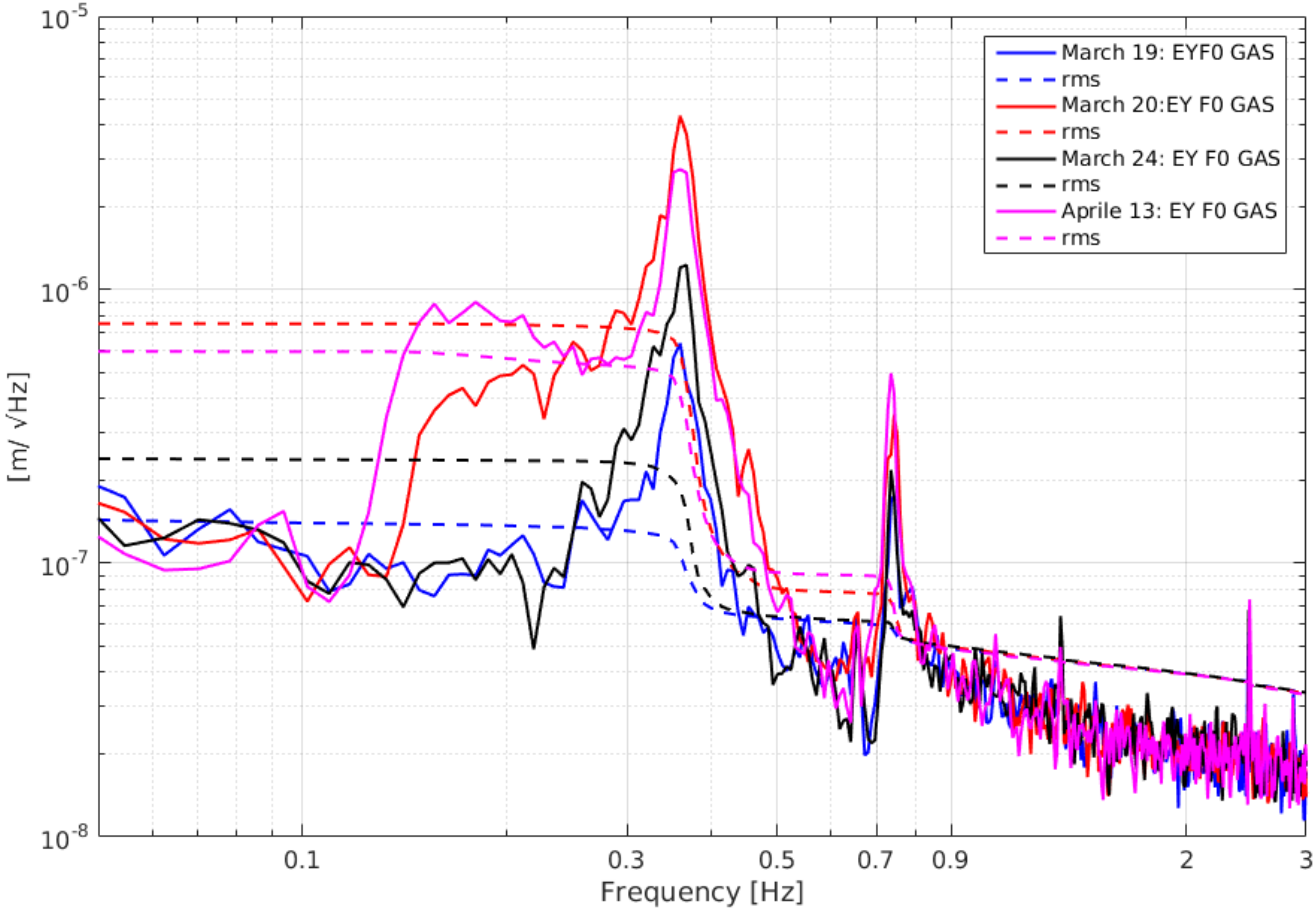

In noisy days the F0 rms is got worse by a factor 6

KAGRA low frequency sensitivity: Type A performance (IV)

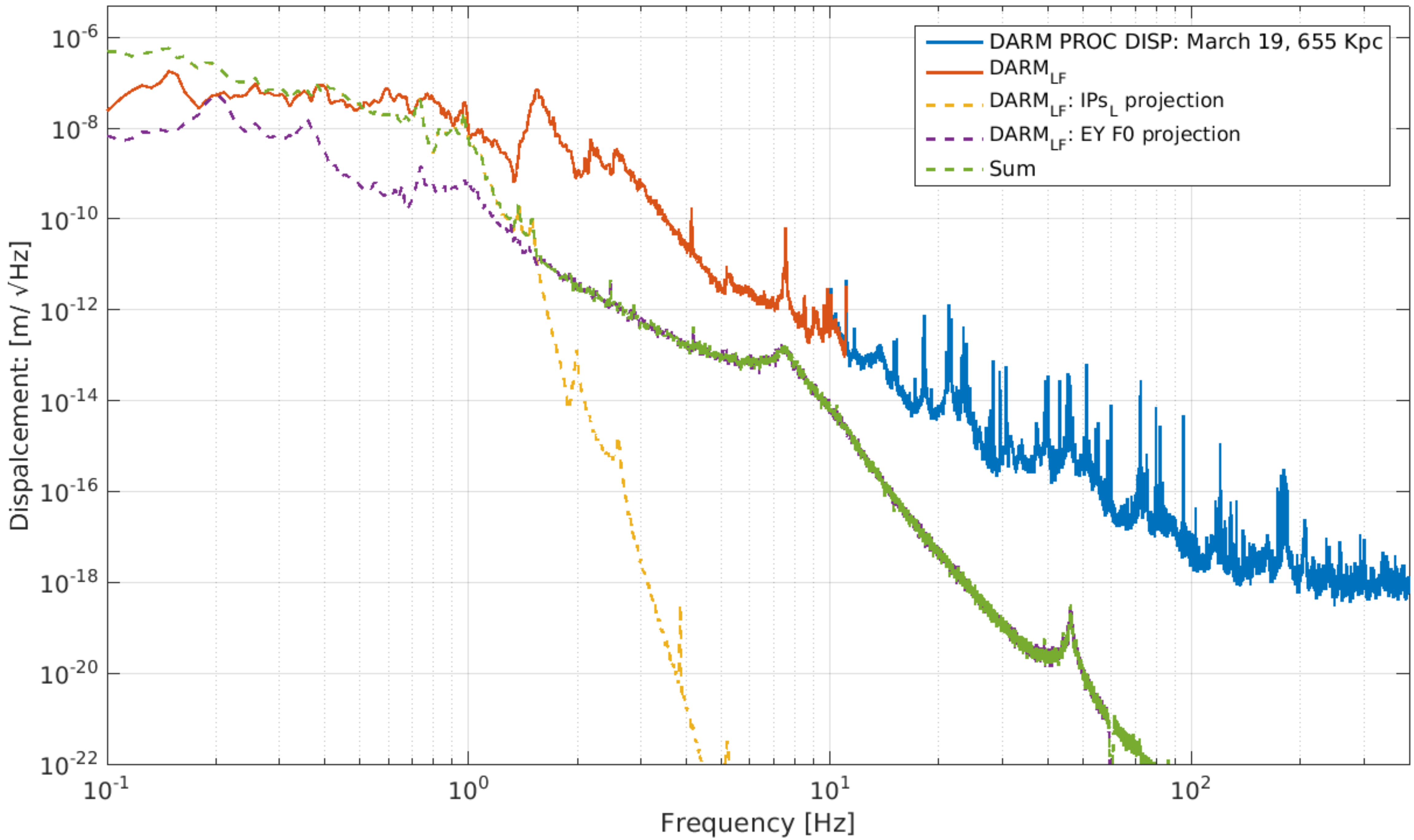

From 0.1 Hz to 0.8 Hz DARM is limited by IP mechanical noise

Above 1 Hz the IP mechanical noise assure a good passive isolation along the L direction

Above 2 Hz the EY vertical mechanical noise became dominant: is not limiting the sensitivity

KAGRA low frequency sensitivity: Type A performance (V)

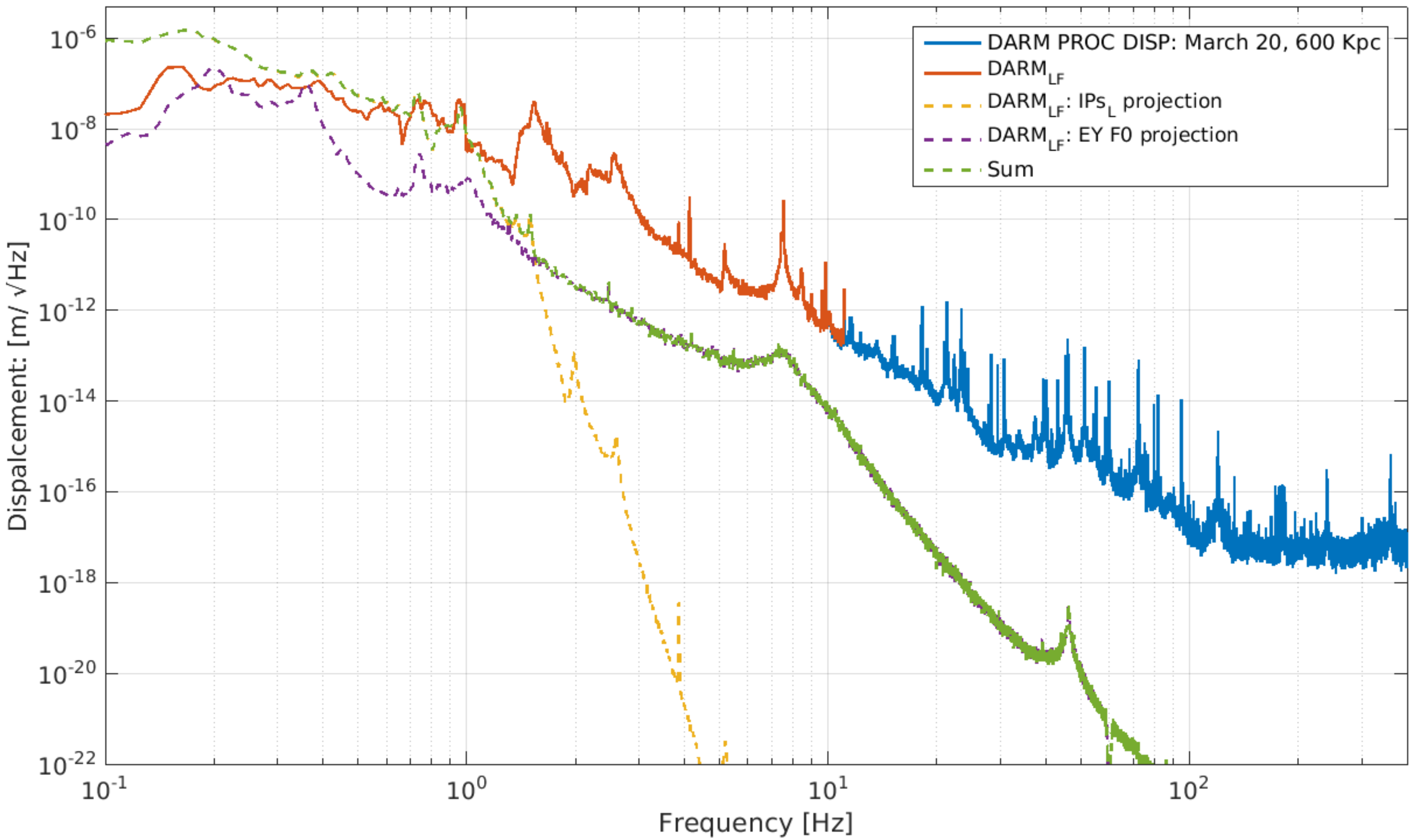

From 0.1 Hz to 0.8 Hz DARM is limited by IP mechanical noise

Above 1 Hz the IP mechanical noise assure a good passive isolation along the L direction

Above 2 Hz the EY vertical mechanical noise became dominant: **not limiting the sensitivity**

KAGRA low frequency sensitivity: Type A performance (VI)

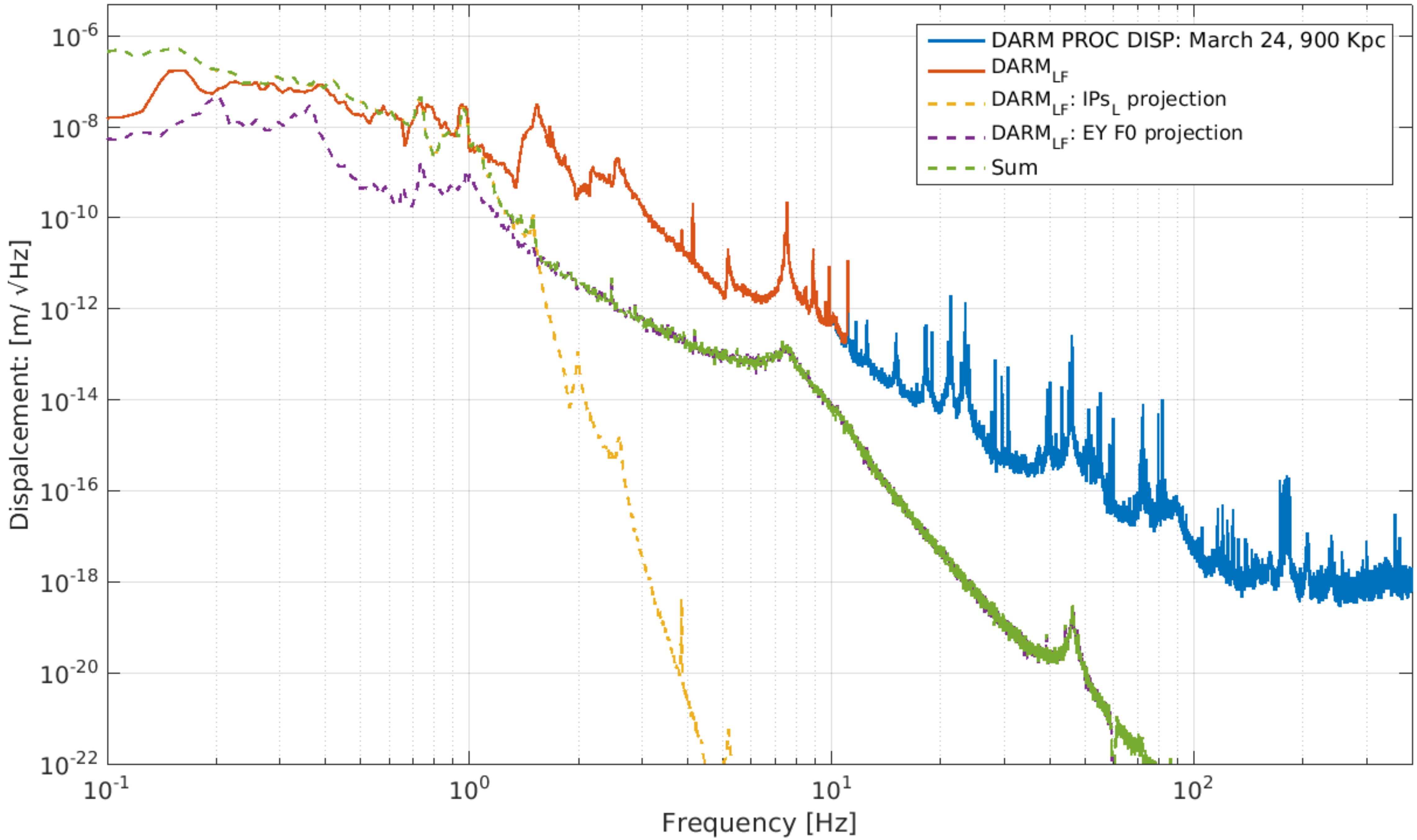

From 0.1 Hz to 0.8 Hz DARM is limited by IP mechanical noise

Above 1 Hz the IP mechanical noise assure a good passive isolation along the L direction

Above 2 Hz the EY vertical mechanical noise became dominant: is not limiting the sensitivity

KAGRA low frequency sensitivity: Type A performance (VII)

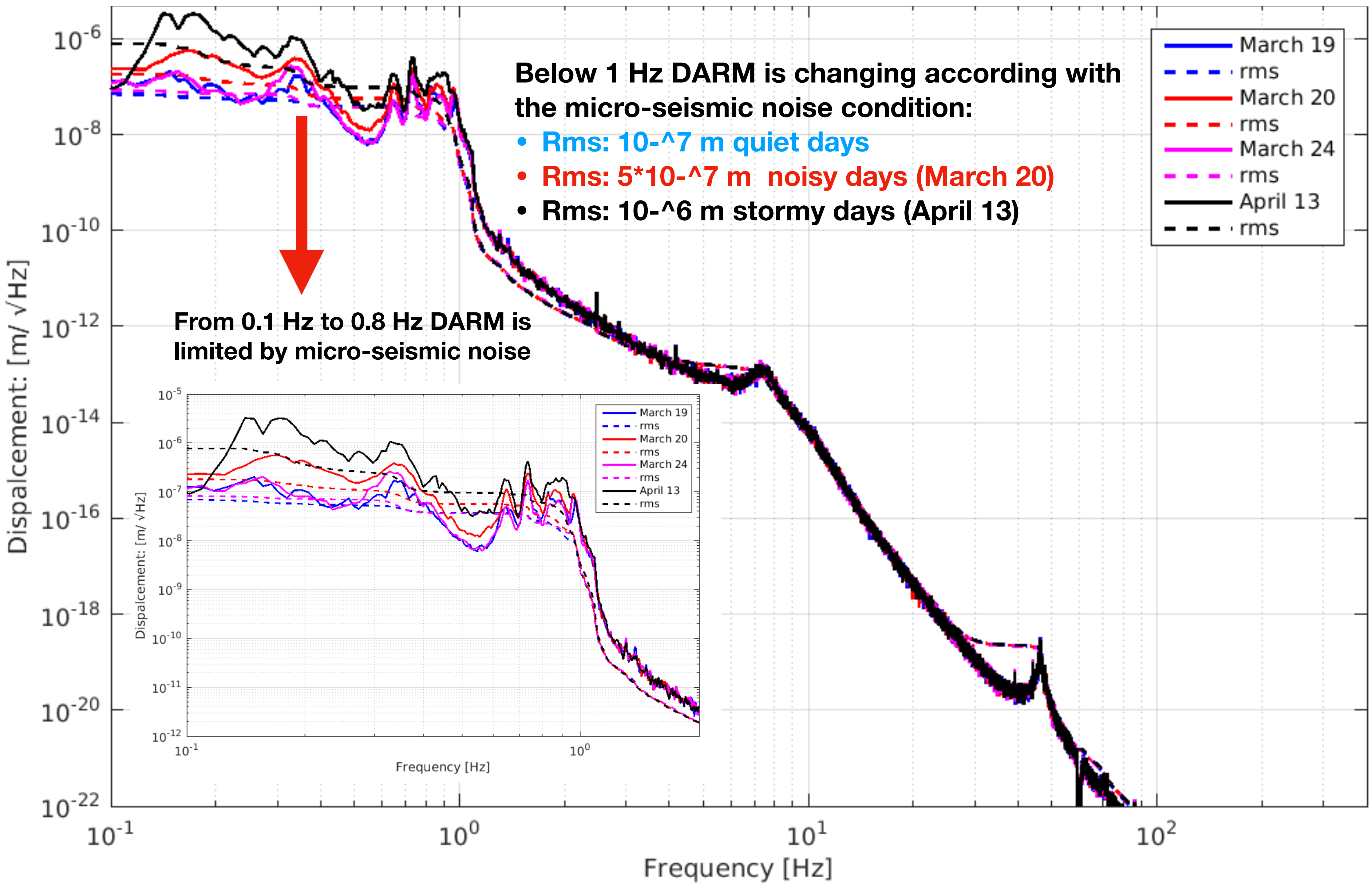

April 13: due to the huge microseismic noise the IFO couldn’t be locked:
DARM fluctuations are 10 times larger than those on quiet days.

What means this in terms of TM_L actuation ?

KAGRA low frequency sensitivity: Type A performance (VIII)

In the current configuration, the feedback force is split through two paths :

MN reallocation scheme:

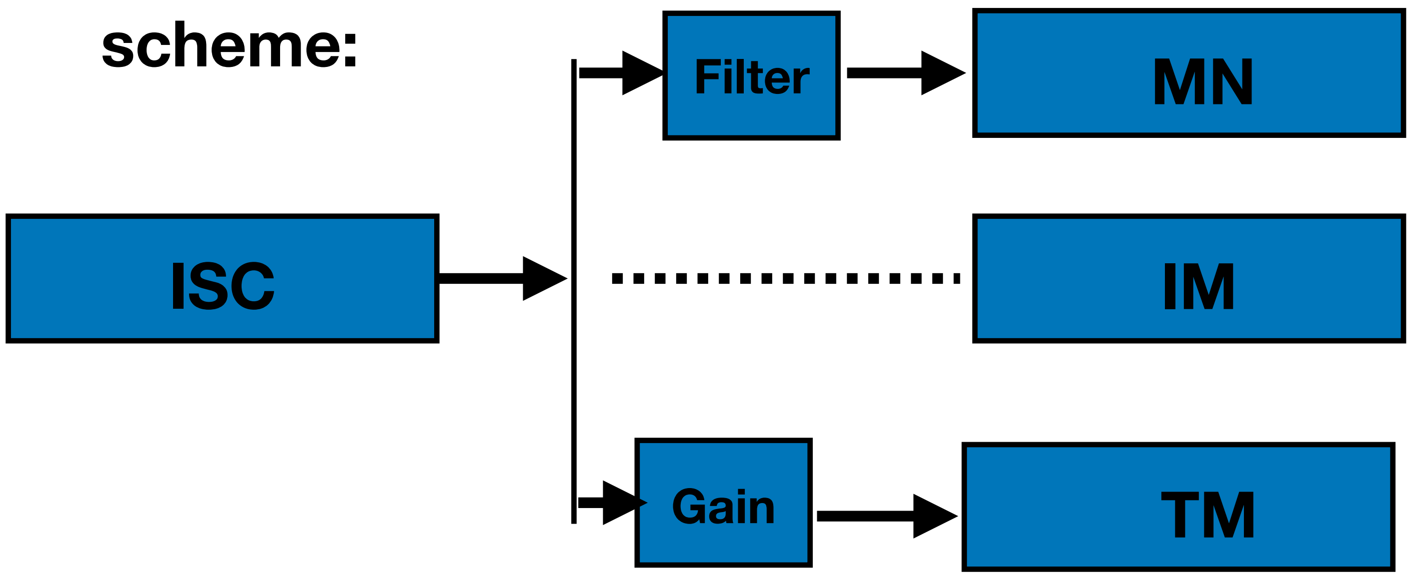

Below 0.1 Hz is sent to the MN actuators

IM: no locking actuations

Above 0.1 Hz is sent to the TM actuators

MN fiter

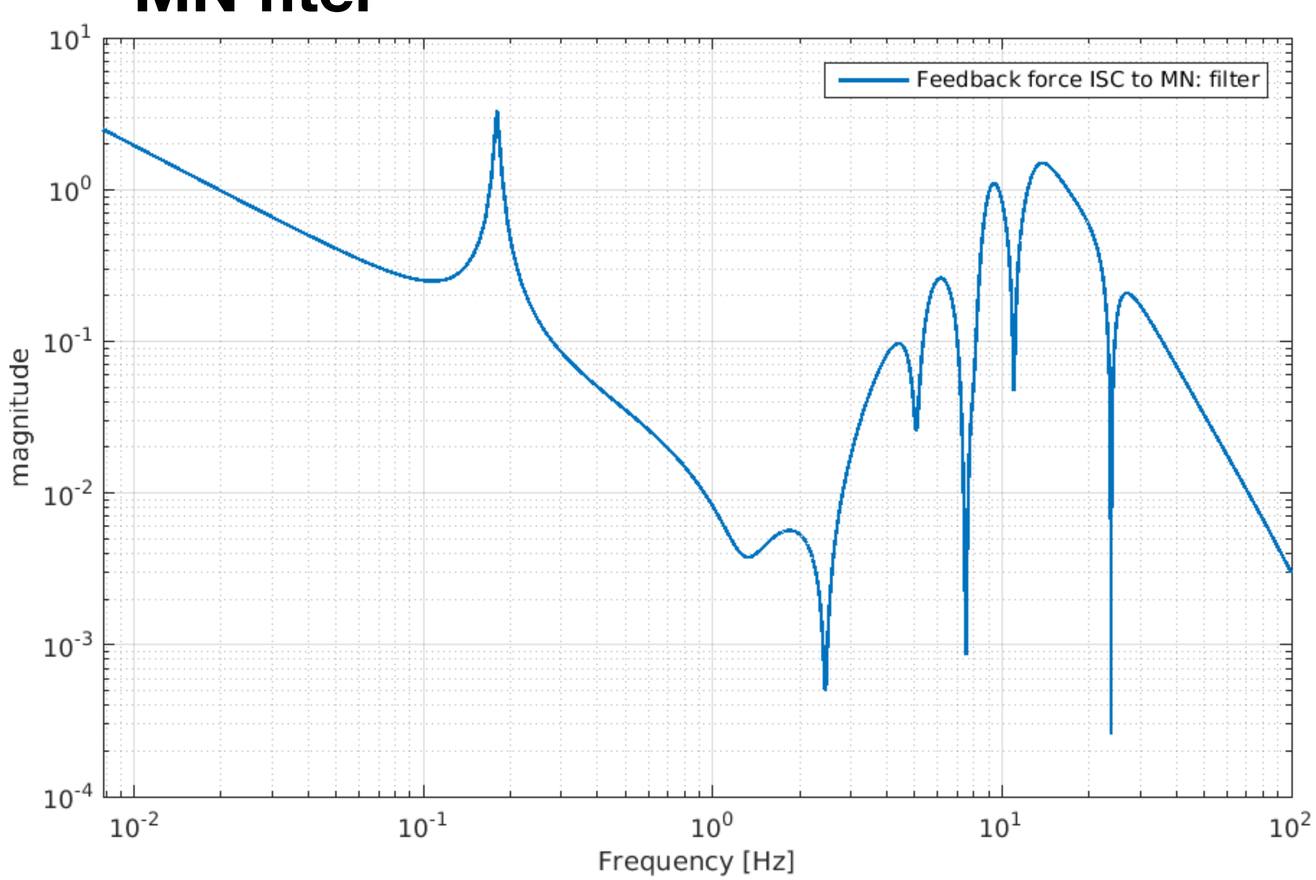

Implemented filter at MN lock stage to change the ISC FB force (TM type) to MN type

KAGRA low frequency sensitivity: Type A performance (IX)

From 0.1 Hz to 0.8 Hz DARM is limited by IP residual motion: $\Delta L_{IP} = \Delta L_{LF}$

Where $\Delta L_{LF}(\omega) = \sqrt{(F_{EX} \cdot M_{EX})^2 + (F_{EY} \cdot M_{EY})^2}$ *and* **F** is the *feedback force sent through the End TMs*

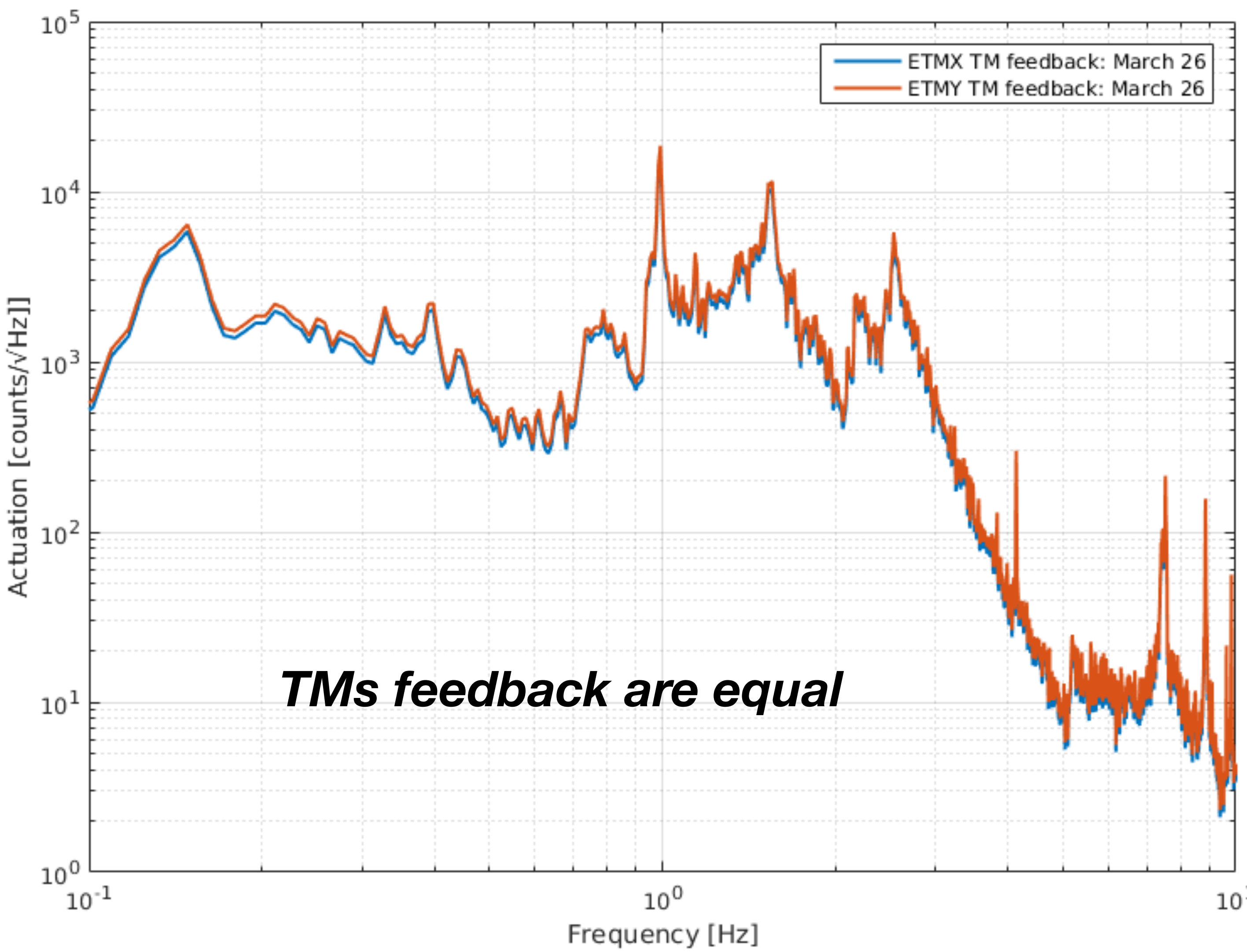

Let's assume that (below 1 Hz):

1) $\Delta L_{IP} = \Delta L_{LF}$

2) $F_{EX} = F_{EY}$

In principle, It is possible to estimate the feedback force as following:

$$F = \frac{\Delta L_{IP}}{\sqrt{2}} \cdot M_{L_{TM}}^{-1}$$

KAGRA low frequency sensitivity: Type A performance (X)

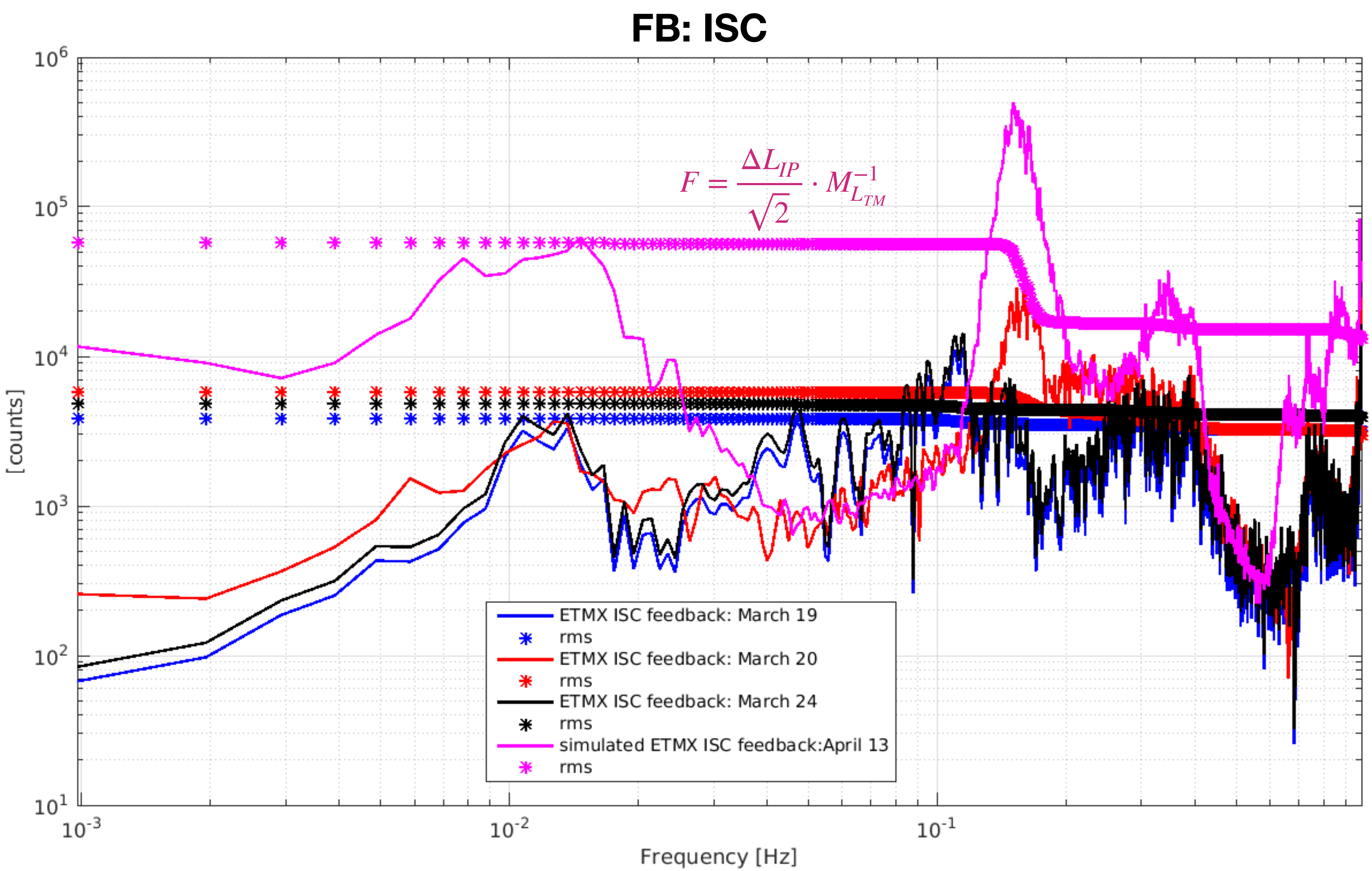

The plot shows how the TM feedback is changing in relation to the micro-seismic noise variation.

March 19: rms= 3000 counts. March 20: rms= 7000 counts. April 13: rms=30000 counts.

KAGRA low frequency sensitivity: Type A performance (XI)

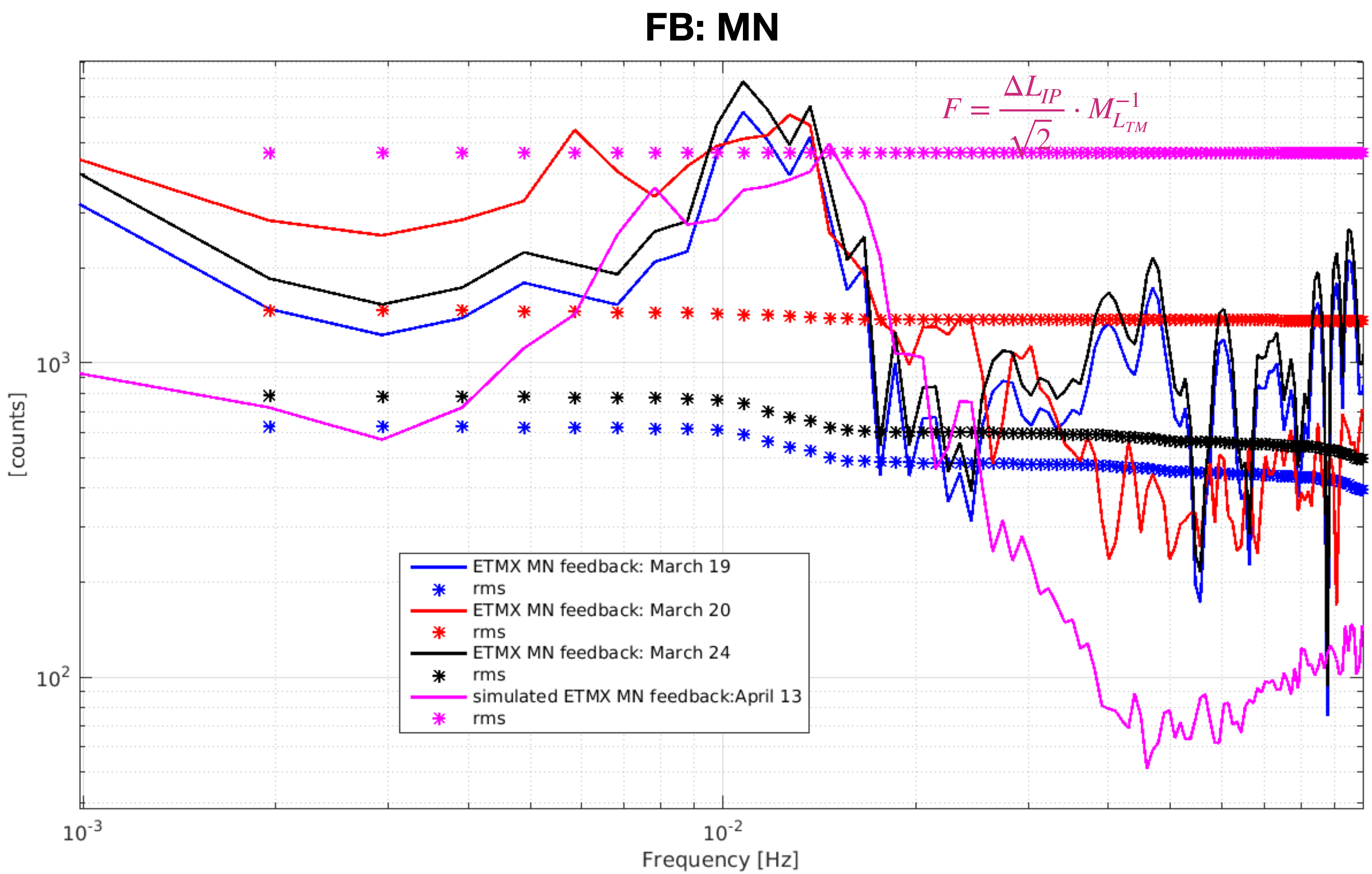

The plot shows how the MN feedback is changing in relation to the micro-seismic noise variation.

March 19: rms= 600 counts. March 20: rms= 1500 counts. April 13: rms=5000 counts.

KAGRA low frequency sensitivity: Type A performance (XII)

Let's focus on the microseismic range and on TM FB:

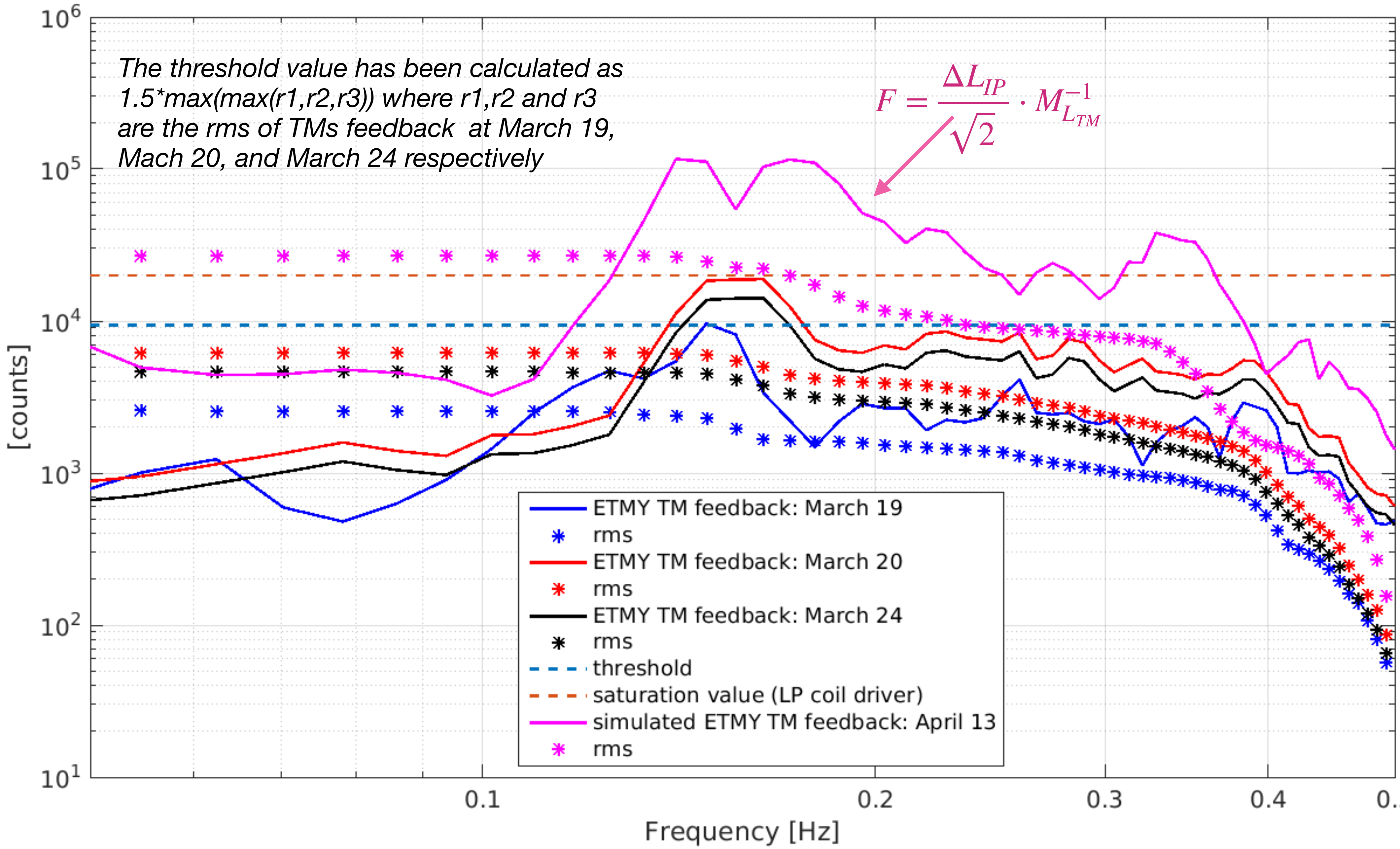

The plot shows how the TM feedback is changing in relation to the micro-seismic noise variation.

March 19: rms= 3000 counts. March 20: rms= 7000 counts. April 13: rms=30000 counts.

On April 13 the IFO has been not locked because the DARM fluctuations were larger than the dynamic range of the TM actuators (rms: 30000 counts).

Conclusions

The performance of the SC, the type A suspensions and their impact on the sensitivity curve when different microseismic conditions occur, during the KAGRA observation run have been analysed.

Interesting microseismic noise levels, have occurred in March 19, March 20 and April 13

On March 19 and on March 20 the IFO (PRFPMI) was locked while on April 13 because of the the huge microseismic noise the IFO couldn't be locked.

The rms of the IP motions, EY_F0 motion , DARM fluctuations and TM feedbacks have changed in relation to the microseismic noise as following:

	March 19	March 20	April 13
Seism	$\sim 10^{-7}$	$\sim 5 \cdot 10^{-7}$	$\sim 2 \cdot 10^{-6}$
IP (m)	$\sim 3 \cdot 10^{-8}$	$\sim 10^{-7}$	$\sim 8 \cdot 10^{-7}$
F0 (m)	$\sim 10^{-7}$	$\sim 2 \cdot 10^{-7}$	$\sim 6 \cdot 10^{-7}$
DARM (m)	$\sim 10^{-7}$	$\sim 5 \cdot 10^{-7}$	$\sim 10^{-6}$
TMs Feedback (counts)	~ 3000	~ 9000	~ 30000

In the stormy days, If the microseismic rms is within [0.8 ,1] micrometer it is possible to lock and to keep the IFO in stable condition for long time (hours) without saturations of the TM actuators.

Conclusions

The performance of the SC, the type A suspensions and their impact on the sensitivity curve when different microseismic conditions occur, during the KAGRA observation run have been analysed.

The analyse shows that with SC and the currents MN reallocation, in the stormy days, If the microseismic rms is within [0.8 ,1] micrometer it is possible to lock and to keep the IFO in stable condition for long time (several hours) without saturations of the TM actuators. When the microseismic rms is greater than 1 micrometer the TM actuation is not enough to compensate the TM fluctuations.

What it could be done to improve the situations?

- **Recover the GAS filters stuck at EY and other TypeAs**
- **Improve the IP control like fine tuning of the SC, IP control filters, etc.**
- **Improve the sensitivity of the inertial sensor below 0.1 to implement a suitable blending technique in order to suppress a factor 3 more the microseismic noise**
- **Extend the control bandwidth on the MN lock to few Hz and use high power coil driver dynamic range to compensate the TM's fluctuations due microseismic noise, in the stormy days**

Thanks for your attention!

Appendix

Type A: SC noise budget (I)

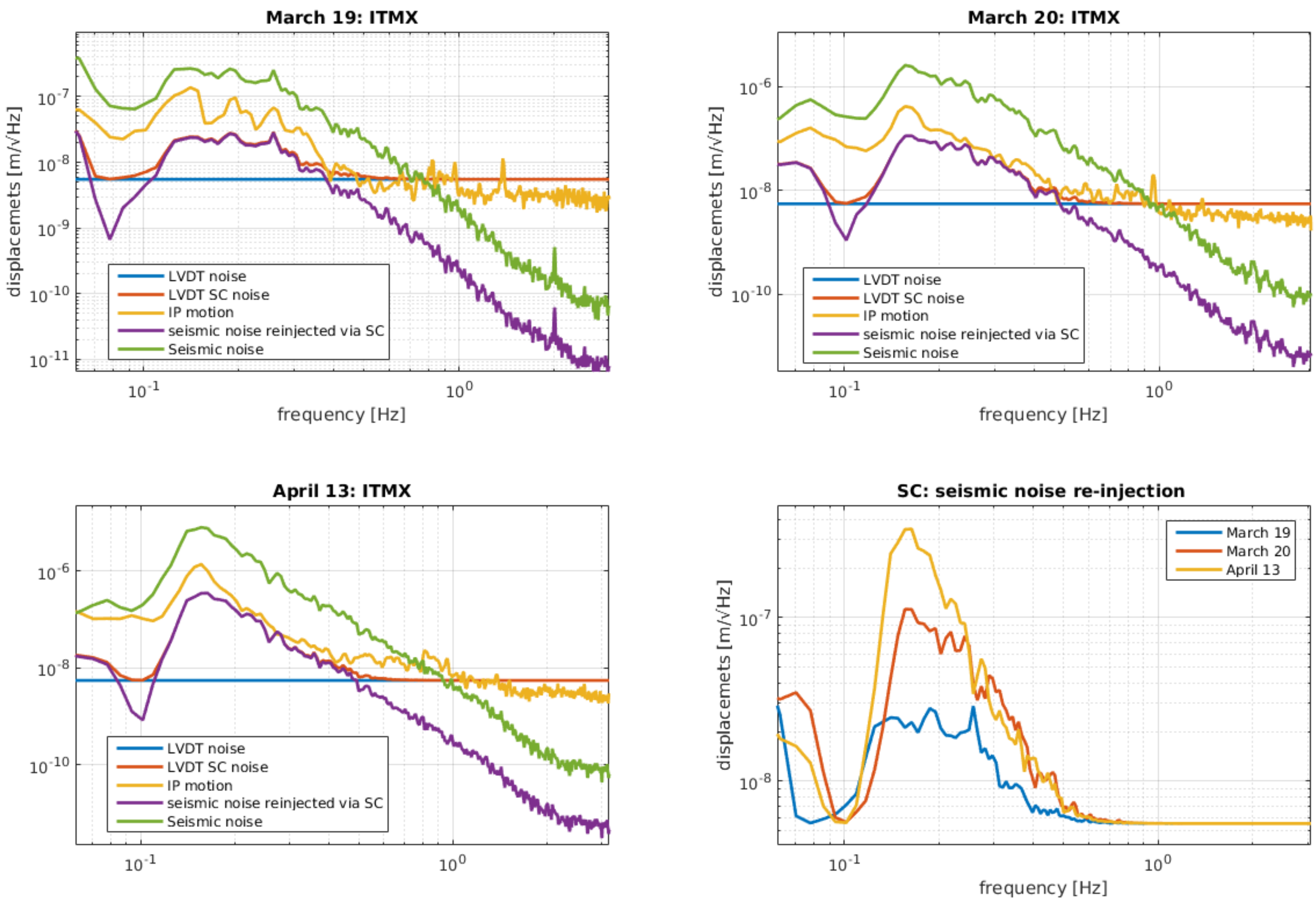

IX : the IP motion is still limited by the seismic noise

Type A: SC noise budget (II)

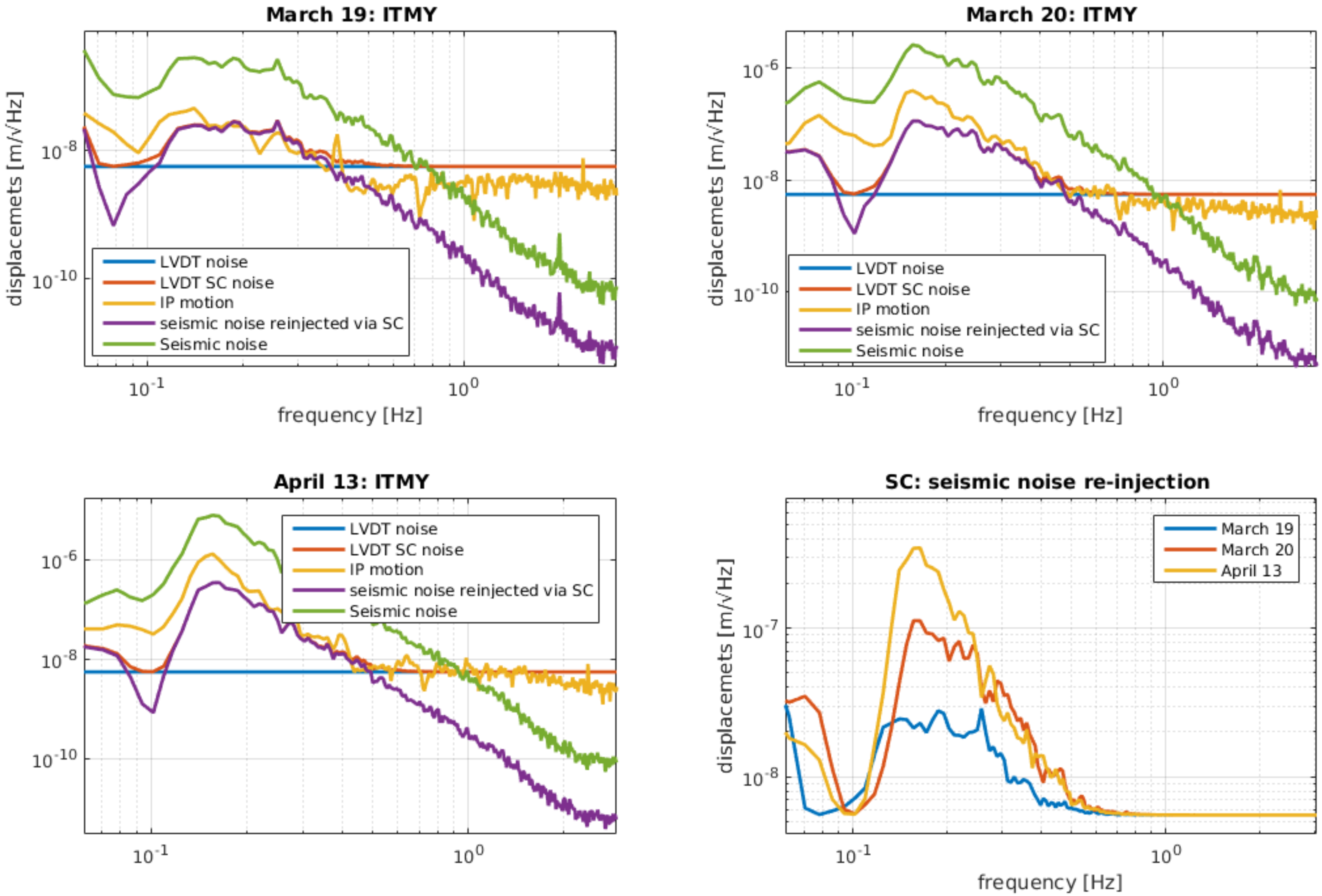

IY : the IP motion is still limited by the seismic noise

Type A: SC noise budget (III)

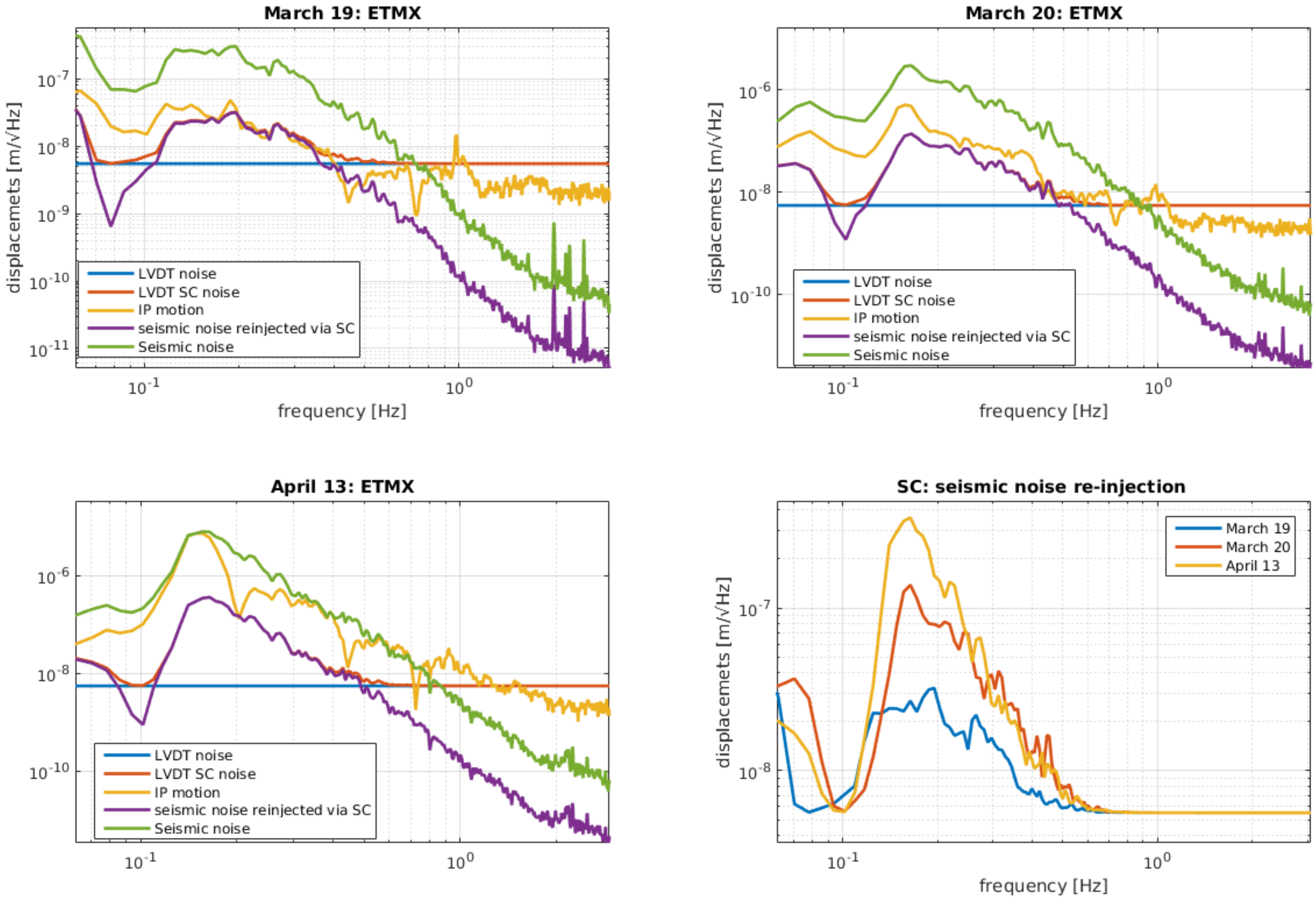

EX : the IP motion is still limited by the seismic noise

Type A: SC noise budget (IV)

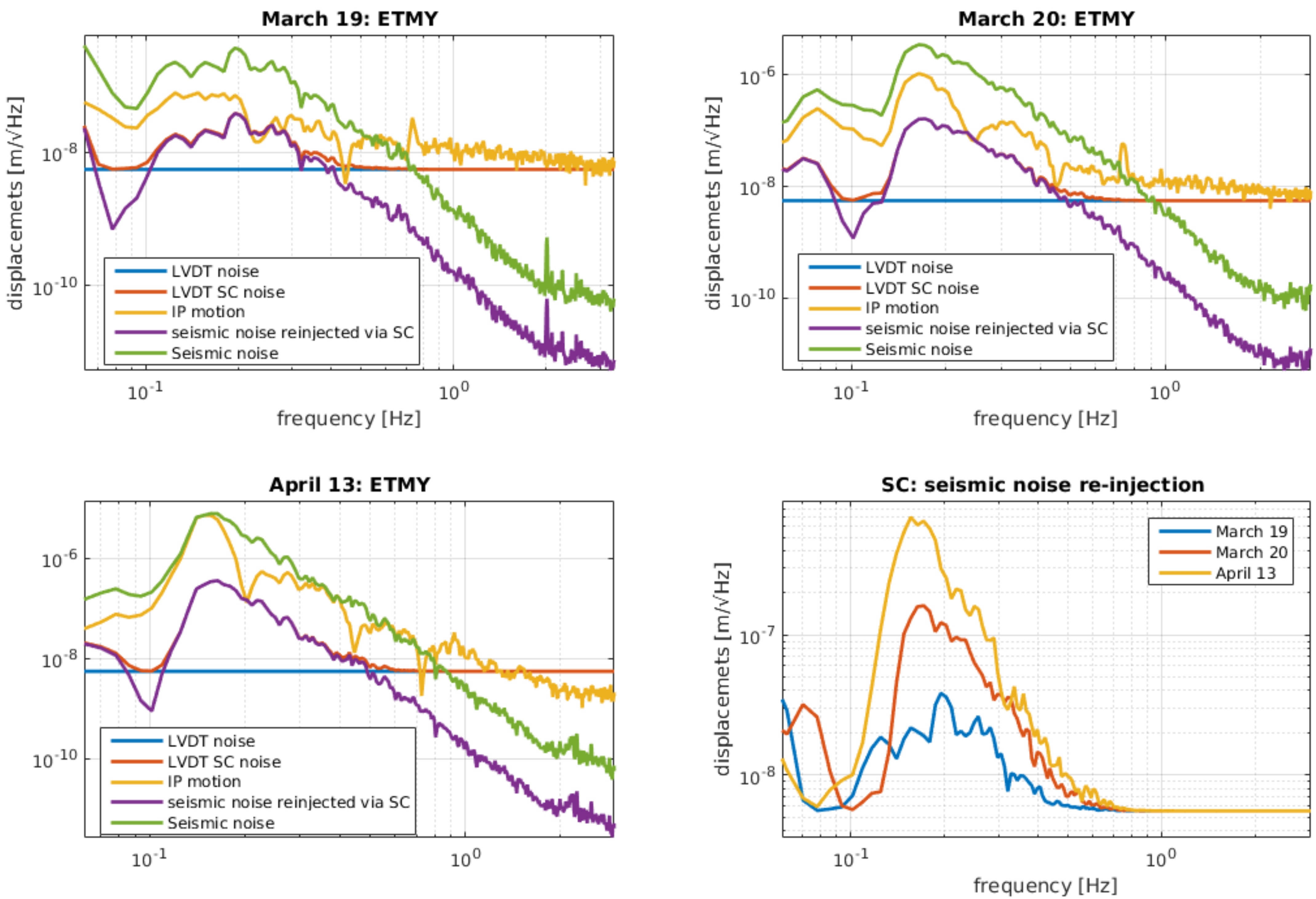

EY: the IP motion is still limited by the seismic noise